Glycoconj J (2010) 27:583–600
DOI 10.1007/s10719-010-9302-5

Thymoquinone-induced Neu4 sialidase activates NFκB in macrophage cells and pro-inflammatory cytokines *in vivo*

Trisha M. Finlay · Samar Abdulkhalek · Alanna Gilmour · Christina Guzzo · Preethi Jayanth · Schammim Ray Amith · Katrina Gee · Rudi Beyaert · Myron R. Szewczuk

Received: 16 March 2010 / Revised: 29 May 2010 / Accepted: 14 July 2010 / Published online: 10 August 2010

Abstract Thymoquinone (TQ) derived from the nutraceutical black cumin oil has been reported to be a novel agonist of Neu4 sialidase activity in live cells (*Glycoconj J DOI* 10.1007/s10719-010-9281-6). The activation of Neu4 sialidase on the cell surface by TQ was found to involve GPCR-signaling via membrane targeting of Gαi subunit proteins and matrix metalloproteinase-9 activation. Contrary to other reports, TQ had no anti-inflammatory effects *in vitro*. Here, we show that MyD88/TLR4 complex formation and subsequent NFκB activation are induced by the Neu4 activity associated with TQ-stimulated live primary bone marrow (BM) macrophage cells from WT and Neu1-deficient mice, HEK-TLR4/MD2 cells and BMC-2 macrophage cell line but not with primary macrophage cells from Neu4-knockout mice. Tamiflu (oseltamivir phosphate), pertussis toxin (PTX), a specific inhibitor of Gαi proteins of G-protein coupled receptor (GPCR) and the broad range inhibitor of matrix metalloproteinase (MMP) galardin applied to live primary BM macrophage cells completely block TQ-induced MyD88/TLR4 complex formation. Using immunocytochemistry and western blot analyses, Tamiflu, galardin and PTX inhibit NFκB activation induced by Neu4 activity associated with TQ-stimulated BMC-2 cells, HEK-TLR4/MD2 cells and primary BM macrophages from WT mice. EMSA analyses on HEK-TLR4/MD2 nuclear cell extracts confirm the nuclear localization and DNA binding of TQ-induced NFκB activation in a biphasic manner within 30 min. Co-immunoprecipitation experiments reveal for the first time that MMP-9 may be an important intermediate link in the

T. M. Finlay · S. Abdulkhalek · A. Gilmour · C. Guzzo · P. Jayanth · S. R. Amith · K. Gee · M. R. Szewczuk (✉)
Department of Microbiology & Immunology, Queen's University, Kingston, ON K7L3N6, Canada
e-mail: szewczuk@queensu.ca

T. M. Finlay
e-mail: tmfinlay@ucalgary.ca

S. Abdulkhalek
e-mail: 9sa22@queensu.ca

A. Gilmour
e-mail: 5amg@queensu.ca

C. Guzzo
e-mail: 3cg8@queensu.ca

P. Jayanth
e-mail: 6pj1@queensu.ca

S. R. Amith
e-mail: ray.amith@ucd.ie

K. Gee
e-mail: kgee@queensu.ca

R. Beyaert
Department for Molecular Biomedical Research, VIB, Unit for Molecular Signal Transduction in Inflammation, Technologiepark 927, 9052 Zwijnaarde, Belgium
e-mail: Rudi.Beyaert@dmbr.vib-UGent.be

R. Beyaert
Department of Biomedical Molecular Biology, Ghent University, Ghent, Belgium

Present Address:
T. M. Finlay
Hotchkiss Brain Institute, University of Calgary, Calgary, Alberta T2N 4N1, Canada

Present Address:
S. R. Amith
Conway Institute, University College Dublin, Belfield, Dublin 4, Ireland

TQ-induced Neu4 activity circuitously targeting TLR4 receptors. Central to this process is that Neu4 forms a complex with MMP-9, which is already bound to TLR4 receptors. Fluorescence spectrophotometer analyses of live CD14-THP1 cells treated with TQ show Neu4 sialidase activity over 5 min. Using flow cytometry analyses, CD14-THP1 cells treated with TQ express stable protein levels of Neu4, TLR4 and MMP9 on the cell surface over 30 min except for a marked diminution of MMP9 at 15 min. Using cytokine array profiling analyses of serum, Neu4-knockout mice respond poorly to TQ in producing pro-inflammatory cytokines and chemokines after 5-h treatment compared to the wild-type or hypomorphic cathepsin A mice with a secondary 90% Neu1 deficient mice. Our findings establish an unprecedented signaling paradigm for TQ-induced Neu4 sialidase activity. It signifies that MMP-9 forms an important molecular signaling platform in complex with TLR4 receptors at the ectodomain and acts as the intermediate link for TQ-induced Neu4 sialidase in generating a functional receptor with subsequent NFκB activation and pro-inflammatory cytokine production *in vivo*.

Keywords Thymoquinone · Cell signaling · Receptor activation · TOLL-like receptor 4 · Neu4 sialidase · Cellular sialidase · NFκB · Cytokines

Abbreviations

TQ	thymoquinone
oseltamivir phosphate	Tamiflu
LPS	lipopolysaccharide
BM	bone marrow
M-CSF	monocyte colony-stimulating factor
4-MUNANA	2′-(4-methylumbelliferyl)-α-D-*N*-acetylneuraminic acid
PVDF	polyvinylidene fluoride
HEK293	human embryonic kidney 293 cells
Neu1 KD	hypomorphic cathepsin A mice with the secondary ~90% reduction of the Neu1 activity
Neu4 KO	Neu4 knockout
EMSA	electrophoretic mobility shift assay

Introduction

TOLL-like receptors (TLR) are highly glycosylated with several N-linked gylcosylation sites located in the inner concave surface of the ectodomain. The precise role of these sugar N-glycans in TLR receptor activation was unknown until now. We recently reported that Neu1 sialidase and not Neu−2, −3 and −4 forms a complex with TLR-2, −3 and −4 receptors on the cell-surface membrane of naïve and activated macrophage cells [1]. Activation of Neu1 is induced by TLR ligands binding to their respective receptors. Endotoxin lipopolysaccharide (LPS)-induced MyD88/TLR4 complex formation and subsequent NFκB activation was also reported to be dependent on the removal of α2-3 sialyl residue(s) linked to β-galactoside of TLR4 ectodomain by the Neu1 activity associated with LPS-stimulated live macrophage and dendritic cells [2]. Taken together, these findings support the premise that Neu1 desialylation of α2-3 sialyl residues of TLR receptors enables removing a steric hinderance to receptor association for TLR activation and cellular signaling.

We also reported an unprecedented activation of Neu4 sialidase on the cell surface of monocytic, dendritic and fibroblast cells by thymoquinone (TQ) [3], which is derived from the nutraceutical black cumin oil. These findings suggested that TQ is a novel agonist of Neu4 sialidase activity in live cells. They also provided evidence for the potentiation of G-protein coupled receptor (GPCR)-signaling via membrane targeting of Gαi subunit proteins and matrix metalloproteinase-9 (MMP-9) activation in inducing Neu4 sialidase by TQ. Central to this process is that Neu4 in alliance with GPCR-signaling Gαi subunit proteins and MMP-9 is expressed on the cell surface of human monocytic THP-1 cells, human WT and WG0544 sialidosis type I fibroblast cells and BMC-2 macrophage cells. This tripartite alliance actually made Neu4 readily available to be induced by TQ because the Neu4 sialidase activity induced by TQ treated live cells occurs within a minute. How Neu4 sialidase is rapidly induced by MMP-9 together with GPCR Gαi subunit proteins remains unknown. Perhaps, it can be speculated that TQ binding to the cell surface GPCR Gαi subunit proteins may lead to GPCR-signaling sufficient to activate MMP. It is well known that agonist-bound GPCRs have been shown to activate numerous MMPs [4], including MMP-3 [5], MMPs 2 and 9 [6, 7], as well as members of the ADAM family of metalloproteases: ADAM10, ADAM15, and ADAM17 [8, 9]. However, the precise molecular mechanism(s) underlying GPCR-mediated MMP activation also remains unknown.

To gain an insight(s) into the properties of TQ-induced Neu4 sialidase activity on the cell surface of macrophage cells, we asked whether TQ-induced Neu4 sialidase activity would actually target TLR receptors, enabling desialylation of TLR receptors and facilitating TLR activation and cellular signaling. The findings in this report indicate this to be the case. TQ-induced Neu4 activity facilitates MyD88/TLR4 complex formation and subsequent NFκB activation and nuclear localization in HEK-TLR4/MD2 cells and primary BM macrophages from WT and Neu1-deficient mice but not in primary

macrophage cells from Neu4-knockout mice. Tamiflu (oseltamivir phosphate), Gαi-sensitive pertussis toxin (PTX) and the broad range inhibitor of matrix metalloproteinase (MMP) galardin applied to live HEK-TLR4/MD2 cells and primary BM macrophage cells completely block TQ-induced MyD88/TLR4 complex formation. The data with co-immunoprecipitation of Neu4 and MMP-9 reveal that Neu4 forms a complex with MMP-9, which is already bound to TLR4. This tripartite alliance would make TQ-induced Neu4 activity readily available to target sialyl residues of TLR4 receptors. In addition, Neu4-knockout mice respond poorly to TQ in producing pro-inflammatory cytokines and chemokines after 5-h treatment compared to the wild-type or hypomorphic cathepsin A mice with a secondary 90% Neu1 deficient mice. The findings in this report suggest that TQ-induced Neu4 sialidase activity on the cell surface circuitously targets TLR4 receptors through a molecular signaling platform of MMP-9 in complex with TLR4 in generating a functional receptor.

Materials and methods

Reagents Thymoquinone (TQ, 99% pure, Aldrich, St. Louis, MO, USA) was reconstituted in 1× Tris buffered saline (TBS) containing 57% dimethyl sulfoxide (DMSO, Bio Shop Canada Inc., Burlington, ON, Canada), and used at indicated optimal dosage as described previously [3]. TLR4 ligand lipopolysaccharide (LPS, 5 μg/mL, from *Serratia marcescens* and purified by phenol extraction; Sigma, St. Louis, MO) and TLR2 ligand, killed *Mycobacterium butyricum* (Myco, 5 μg/mL, DIFCO) were used at indicated optimal dosage.

The sialidase substrate, 2′-(4-methylumbelliferyl)-α-D-*N*-acetylneuraminic acid (98% pure, 4-MUNANA, Biosynth International Inc., Itasca, IL, USA) was used at optimal concentration of 0.318 mM for the live cell sialidase assay as described previously [1–3].

Tamiflu (99% pure oseltamivir phosphate, Hoffmann-La Roche Ltd., Mississauga, Ontario, Lot # BS00060168) was used at indicated concentrations.. Pertussis toxin (PTX, from *Bordatella pertussis*, in buffered aqueous glycerol solution, Sigma-Aldrich Canada Ltd., Oakville, Ontario, L6H 6J8) catalyzes the ADP-ribosylation of the α subunits of the heterotrimeric G proteins G_i, G_o, and G_t. This prevents the G protein heterotrimers from interacting with receptors, thus blocking their coupling and activation. Galardin (GM6001; molecular formula $C_{20}H_{28}N_4O_4$, *N*-[(2*R*)-2-(Hydroxamidocarbonylmethyl)-4-methylpentanoyl]-L-tryptophan methylamide; Cat.# 364205, Calbiochem-EMD Chemicals Inc., Darmstadt, Germany) is a potent, cell-permeable, broad-spectrum hydroxamic acid inhibitor of matrix metalloproteinases (MMPs); (IC_{50}=400 pM for MMP-1; IC_{50}=500 pM for MMP-2; IC_{50}=27 nM for MMP-3; IC_{50}=100 pM for MMP-8; and IC_{50}=200 pM for MMP-9).

Cell lines BMC-2 or BMA macrophage cells [10] were obtained from Dr Ken L. Rock, University of Massachusetts Medical School, Worcester, MA. Stable HEK-TLR4 cells were obtained by calcium phosphate transfection of a pCDNA3 expession vector for a specific chimeric TLR4 with an in frame C-terminal YFP and selection in 0.8 μg/ml G418. The HEK-TLR4/MD2 cell line was generated by additional co-transfection of an expression plasmid for human MD2. All cells were grown at 37°C in 5% CO_2 in culture media containing DMEM (Gibco, Rockville, MD) supplemented with 5% horse serum (Gibco) and 3% fetal calf serum (FCS) (HyClone, Logan, Utah, USA). THP-1 cells, a promonocytic cell line, were transfected with a plasmid containing CD14 cDNA sequences (CD14-THP1) as described elsewhere [11]. CD14-THP1 cells were cultured in Iscove's modified Dulbecco's medium (Sigma) supplemented with 10% FCS and selection in 100 μg/ml G418.

Mouse models Wild-type (WT), Neu4 KO (Neu4 knockout) [12] and Neu1-CathA KD (Neu1 deficient and cathepsin A deficient) [13] mice were obtained from Dr. Alexey Pshezhetsky's laboratory (Departments of Pediatrics and Biochemistry, Montreal University, Service de Genetique, Ste-Justine Hospital, 3175 Cote-Ste-Catherine, H3T1C5, Montreal, QC, Canada). The Neu1-CathA KD mice have a hypomorphic cathepsin A phenotype with a secondary ~90% reduction of the Neu1 activity [13].

Primary mouse bone marrow macrophage cells Bone marrow (BM) cells were flushed from femurs and tibias of mice with sterile Tris-buffered saline (TBS) solution. The cell suspension was centrifuged for 3 min at 900 rpm, and the cell pellet resuspended in red cell lysis buffer for 5 min. The remaining cells were washed once with sterile TBS, and then resuspended in RPMI conditioned medium supplemented with 10% FCS and 20% (v/v) of L929 cell supernatant as a source of monocyte colony-stimulating factor (M-CSF) according to Alatery and Basta [14] and 1× L-glutamine-penicillin-streptomycin (Sigma-Aldrich Canada Ltd., Oakville, Ontario) in sterile solution. The primary BM macrophages were grown on 12 mm circular glass slides in RPMI conditioned medium for 7–8 days in a humified incubator at 37°C and 5% CO_2. By day 7 these primary macrophage cells are more than 95% positive for macrophage marker F4/80 molecule as detected by flow cytometry [14].

Fluorescence spectrophotometer analysis of TQ-induced sialidase activity in cell suspensions of human monocytic CD14-THP1 cells Cells at 90% confluence in 25-cm^2

flasks were resuspended in 5 mL of serum-free Tris-buffered medium pH7.4. To 50 μL of cell suspension (0.5 or 1.0×10^6 cells/mL) in MicroFluor black 96-well flat bottom microtiter plates (Thermo Electron, Fisher Scientific Company, Ottawa, Ontario, K2E 7 L6) was added 0.318 mM final concentration of 4-MUNANA with or without the presence of 100 μg/mL TQ. The fluorescence intensity readings were immediately taken over 4.5 min using the Varioskan Fluorescence Spectrophotometer (Type 3001, Microplate Instrumentation, Thermo Electron Corporation, Vantaa, Finland) at emission 450 nm following an excitation at 365 nm. The sialidase activity in the live cell samples corrected for background endogenous sialidase activity in untreated cells was calculated from a standard neuraminidase activity curve, and expressed as milli Units per mg of 4-MUNANA for the indicated cell concentrations.

NFκB activation HEK-TLR4/MD2 cells were treated with either TLR4 specific endotoxin lipopolysaccharide (LPS) for 15–45 min or TQ for 15–60 min. Cells were fixed, permeabilized, and immunostained with rabbit anti-NFκBp65 or rabbit anti-IκBα antibodies followed with Alexa Fluor594 goat anti-rabbit IgG. In addition, cells were fixed, permeabilized, and immunostained with phospho-specific polyclonal rabbit antibody against the human NFκB p65 (Rel A) phospho specific pS529 (pNFκB; Rockland Immunochemicals, Inc., Gilbertsville, PA) with minimal reactivity with non-phosphorylated p65 followed with Alexa Fluor594 goat anti-rabbit IgG. Stained cells were visualized by epi-fluorescence microscopy using a 40× objective. Quantitative analysis was done by assessing the density of cell staining corrected for background in each panel using Corel Photo Paint 8.0 software. Each bar in the figures represents the mean corrected density of staining ± SEM for all cells within the respective images.

Nuclear extracts and electrophoretic mobility shift (EMSA) Nuclear extracts of HEK-TLR4/MD2 cells were prepared by harvesting the cells before and after treatment with TQ as described. Cells were lysed in a buffer consisting of 100 mM HEPES (4-(2-hydroxyethyl)-1-piperazineethanesulfonic acid), 100 mM KCl, 100 EDTA (ethylenediamine tetraacetic acid), 100 mM DTT (dithiothreitol), protease inhibitors and 10% NP-40 (Nonidet-P40). The lysates were incubated on ice for 10 min and centrifuged at 13,000 rpm for 3 min. The pellets were resuspended in 100 mM Hepes, 2 M NaCl, 5 mM EDTA and 50% glycerol, incubated on ice again for 2 h and then centrifuged at 13,000 rpm for 5 min. The supernatant containing the nuclear extracts were stored at −80°C.

Electrophoretic mobility shift assay (EMSA) detects NF-κB DNA binding activity using a 3′ biotinylated double-stranded oligonucleotide sequence 5′ AGT TGA GGG GAC TTT CCC AGG C 3′ (Operon Biotechnologies Inc., Huntsville, AL) against the NF-κB binding site. The reaction volumes were 20 μl comprising of 20 μg of nuclear extract incubated at room temperature for 30 min with 5 ng of the biotinylated oligonucleotide probe in binding buffer (Pierce Lightshift Chemiluminescent EMSA kit, Rockford, USA). The NF-κB bound to oligonucleotide was resolved on a 5% polyacrylamide gel in Tris/Glycine running buffer at 20 mA constant current. The gel was transferred onto a PVDF membrane and cross-linked by UV radiation for 3 min. The blot was probed with Streptavidin-HRP at a dilution of 1:300 for 15 min at room temperature followed with Western Lighting Chemiluminescence (PerkinElmer Life Sciences, Boston). For supershift of nuclear NFκB, supernatants containing the nuclear extracts from TQ-treated HEK-TLR4/MD2 cells at different time intervals were analyzed by EMSA to detect NF-κB DNA binding activity using a 3′ biotinylated double-stranded oligonucleotide (oligo) sequence 5′ AGT TGA GGG GAC TTT CCC AGG C 3′ against the NF-κB binding site. Non-biotinylated oligo probe was used as a NF-κB binding competitor. Anti-NFκBp65 antibody at 5 μg/μL, 250 μg/μL and 500 μg/μL was used to block NF-κB binding to probe. The blot was probed with Streptavidin-HRP followed with Western Lighting Chemiluminescence (PerkinElmer Life Sciences, Boston).

Co-immunoprecipitation and Western blots Primary BM macrophages or HEK-TLR4/MD2 cells are left cultured in media, pretreated with 200 μg/mL Tamiflu for 30 min or in media containing 100 μg/mL TQ for 5 min. Cells (1×10^7 cells) are pelleted and lysed in lysis buffer (50 mM Tris, pH 8, 150 mM NaCl, 1% NP-40, 0.2 mg/ml leupeptin, 1% β-mercaptoethanol, and 1 mM phenylmethanesulfonyl fluoride (PMSF)). Cell lysate proteins are resolved by 8% gel electrophoresis (SDS-PAGE). Proteins are transferred to polyvinylidene fluoride (PVDF) transfer membrane blot. The blot is probed for NFκB pS529 (65 kDa) with anti-pS529 antibody (Rockland Immunochemicals, Inc.) followed by HRP conjugated secondary IgG antibody and Western Lightning Chemiluminescence Reagent Plus. The initial blot is stripped and further probed for β-actin with monoclonal mouse anti-β-actin (Sigma-Aldrich Canada Ltd., Oakville, Ontario). For immunoprecipitation, Neu4, MMP-9, and TLR4 in cell lysates from HEK-TLR4/MD2 cells are immunopreciptated with either 0.69, 0.35 and 0.17 μg of rabbit anti-human Neu4, 1.0, 0.5 and 0.25 μg of rabbit anti-human MMP-9, 2 μg of mouse anti-human TLR4 antibodies or 2 μg of IgG isotype control for 24 h. Following immunoprecipitation, complexes are isolated using protein A or G magnetic beads, washed 3× in buffer (10 mM Tris, pH8, 1 mM EDTA, 1 mM EGTA, 150 mM

NaCl, 1% Triton X-100 and 0.2 mM sodium orthovanadate) and resolved by 8% gel electrophoresis (SDS-PAGE). Proteins are transferred to polyvinylidene fluoride (PVDF) transfer membrane blot. The blots are probed for either Neu4 (53 kDa) with anti-Neu4 (ProteinTech Group, Inc., Chicago, USA), MMP-9 (78 or 84 kDa active) with anti-MMP-9 (H-129, Santa Cruz Biotechnology, Inc. CA) or TLR4 (88 kDa) with anti-human TLR4 (HTA125, Santa Cruz) followed by HRP conjugated secondary IgG antibodies or Clean-Blot IP Detection Reagent for IP/Western blots (Pierce Biotechnology, Thermo Fisher Scientific, Rockford, IL) and Western Lightning Chemiluminescence Reagent Plus. The chemiluminescence reaction was analyzed with x-ray film. Sample concentration for gel loading was determined by Bradford reagent (Sigma-Aldrich Canada Ltd., Oakville, Ontario).

MyD88 colocalization with TLR4 Primary BM macrophages obtained from normal, wild-type (WT), Neu1-CathA KD (Neu1 deficient and cathepsin A deficient) or Neu4 KO (Neu4-knockout) mice were cultured in RPMI medium supplemented with 20% M-CSF, 10% FCS and Penn/Strep/Glut for 8 days on circular glass slides in 24 well tissue culture plates. HEK-TLR4/MD2 cells were cultured in DMEM medium with 10% FCS and 100 μg/mL G418 selection reagent. Cells were pretreated with either 400 μM Tamiflu, 500 nM galardin or 100 ng/ml pertussis toxin (PTX) for 5 min followed with either 5 μg/mL LPS for 5 min, 100 μg/mL TQ for 5 min or left untreated as controls. Cells were fixed, permeabilized, and immunostained with rabbit anti-MyD88 (HFL-296, Santa Cruz Biotech, Santa Cruz, CA, USA) or rat anti-TLR4/MD2 (MTS510, Santa Cruz Biotech) followed with Alexa Fluor594 goat anti-rabbit IgG or Alexa Fluor488 rabbit anti-rat IgG. Stained cells were visualized using a confocal inverted microscope (Leica TCS SP2 MP inverted Confocal Microscope) with a 100× oil objective. Images were captured using a z-stage of 8–10 images per cell at 0.5-mm steps and were processed using Image J 1.38× software (NIH, USA). To calculate the amount of colocalization in the selected images, the Pearson correlation coefficient was measured and expressed as a percentage using Image J 1.38× software.

Cell viability BMA cells were grown overnight in 24 well plates on 12 mm circular glass cover slides in DMEM medium containing 5% fetal bovine serum at 37°C in 5% CO_2. After removal of medium, cells were left untreated as no ligand control or pretreated with 400 μM Tamiflu, 500nM Galardin, or 100 ng/ml Pertussis toxin (PTX) for 30 min followed with 200 μg/mL TQ for 30 min. Positive control for non-viable cells was treated with 100 μl of 1 mM hydrogen peroxide (H_2O_2) 30 min at 37°C. Stain mixture for cell viability was prepared using 1 μL of 200 μg/mL acridine orange and 1 μL of 200 μg/mL ethidium bromide solution (Sigma-Aldrich) in 998 μL of sterile 1× TBS. After removing media or reagents, cells on circular glass slides were quickly rinsed in 1× Tris buffered saline and added to 1 μL of stain mixture mixed with 4 μL of fluorescence mounting medium (DAKO, USA). This stain combination shows non-viable cells to appear red and viable cells, green. Stained cell images were taken using epi-fluorescent microscopy (40× objective).

Flow cytometry of cell surface Neu4 and MMP-9 in live human monocytic CD14-THP-1 cells Cells were grown in 25-cm^2 flasks at 90% confluence. For cell surface staining, live cells in serum free cold phosphate-buffered saline (PBS) were stained for Neu4 (53 kDa) with PerCP/Cy5.5 tandem conjugated rabbit polyclonal anti-Neu4 (ProteinTech Group, Inc., Chicago, USA), R-Phycoerythrin (R-PE) conjugated anti-CD14 antibody or fluorescein conjugated anti-TLR4 antibody for 30 min on ice. Lightning-link™ PerCP-Cy5.5 tandem conjugation kit (Innova Biosciences Ltd., Cedarlane Canada, Burlington, Ontario, Canada L7L 5R2) was used to conjugate the primary antibody as described above. The PerCP is excited at 482 nm and functions as an energy donor for the Cy5.5. Energy is transferred from the PerCP to the Cy5.5 via energy resonance transfer. The Cy5.5 emits the energy received from the PerCP in the form of long wavelength light at 700 nm. After washing with cold PBS buffer, the cells were prepared for flow cytometry analysis. 15,000 cells were acquired on a Beckman Coulter (Miami, FL) Epics XL-MCL flow cytometer and analyzed with Expo32 ADC software (Beckman Coulter). The mean channel fluorescence (MCF) for each histogram is indicated for 50% gated cells.

Cytokine array profiling Mice were bled before (no TQ) and 5 h after i.p. injection with 2.5 mg of TQ per mouse. Serum was extracted and immediately analyzed for cytokine array profiling with R&D System Cytokine Array Profiling ARY066 kit (R&D Systems, Inc., Minneapolis) according to kit protocol. The chemiluminescence reaction is analyzed with either a Fluorochem HD2 Imaging System (Alpha Immunotech, San Leandro, CA, USA) or x-ray film. For x-ray film, quantitative analysis was done by assessing the density of staining corrected for background in each spot using Corel Photo Paint 8.0 software.

RNA isolation and reverse transcriptase PCR Total RNA was extracted from HEK-TLR4/MD2 cell pellets using TRI Reagent RNA Isolation Reagent (Sigma-Aldrich Canada Ltd., Oakville, Ontario L6H 6J8). RNA measurement was performed using the ND-1000 (NanoDrop Technologies,

Wilmington, DE 19810, USA) spectrophotometer. RNA (2 μg) was reverse transcribed using the Moloney Murine Leukemia Virus Reverse Transcriptase Enzyme (Invitrogen). Equal aliquots of cDNA (2 μL) were used for β-actin (660 bp, 40 cycles), IL-6 (295 bp, 40 cycles), TNF-α (413 bp, 30 cycles) and MIP-1β (295 bp, 40 cycles). Primers were diluted in RNase free water according to specifications. Primers used were acquired from Integrated DNA Technology, Coralville, IA and they were: β-Actin: (660 bp) Forward 5′-TGA CGG GGT CAC CCA CAC TGT GCC CAT -3′ Reverse 5′-CTA GAA GCA TTT GCC GAC GAT GGA GGG-3′; IL-6: (295 bp) Forward 5′-GAA CTC CTT CTC CAC AAG CG-3′ Reverse 5′-GAA TCC AGA TTG GAA GCA TCC-3′; TNF-α: (413 bp) Forward 5′-GAG TGA CAA GCC TGT AGC CCA TGT TGT AGC-3′ Reverse 5′-GGC AAT GAT GAT CCC AAA GTA GAC CTG CCC AGA CT-3′; MIP-1β: (214 bp) Forward 5′-TGT CTC TCC TCA TGC TGA TG-3′ Reverse 5′-GTA CTC CTG GAC CCA GGA T-3′. Diluted primers were then added to 2 μl of cDNA and 3 μl of 5× Taq Polymerase Master Mix (New England BioLabs Inc.). DNA mixture was placed in the thermocycler (Thermo Electron Corporation) on a cycling program dependent on primer. The amplified products were resolved by electrophoresis on 1.2% agarose gels and visualized by UV detection of ethidium bromide intercalation on the Alpha Innotech HD2 Imager (Alpha Innotech, Cell Biosciences, Inc., Santa Clara, CA).

Results

Thymoquinone (TQ) induces NFκB activation in HEK-TLR4/MD2 cells and primary bone marrow (BM) macrophages

We have reported that endotoxin lipopolysaccharide (LPS)-induced MyD88/TLR4 complex formation and subsequent NFκB activation is dependent on the removal of α2-3 sialyl residues linked to β-galactoside of TLR4 by the Neu1 sialidase activity [1, 2]. Activation of Neu1 is induced by TLR ligands binding to their respective receptors. Central to this premise is that Neu1 sialidase and not Neu−2, −3 and −4 forms a complex with TLR-2, −3 and −4 receptors on the cell surface membrane of naïve and activated macrophage cells [1]. We have also reported that TQ induces Neu4 sialidase activity on the cell surface of macrophage, dendritic and fibroblast cells [3]. Since Neu1 and Neu4 mammalian sialidases have similar enzymatic functions [15], we asked whether TQ-induced Neu4 activation would actually target the glycosylated TLR4 receptors to facilitate receptor activation and subsequent NFκB activation. To test this hypothesis, we used TLR4-deficient HEK-293 cells stably transfected with human TLR4 and MD2. Immunocytochemistry analyses shown here demonstrate that TQ-treatment of HEK-TLR4/MD2 cells induces NFκB activation (Fig. 1a) with a loss of IκBα within 15 min with a concomitant diminution of NFκB activation after 60 min. The anti-NFκB p65 (Rel A) antibody used here detects activated and non-activated NFκB. In these experiments, we also used anti-IκBα antibody in conjunction with anti-NFκB p65 (Rel A) antibody as an internal control for NFκB activation. IκBα binds to the p65 subunit, preventing nuclear localization and DNA binding. Activation of NFκB releases IκBα bound to p65 subunit and it becomes degraded. For the LPS treated cells, there was an increase in LPS-induced NFκB activation within this same time interval used for TQ.

Using electrophoretic mobility shift assay (EMSA), the nuclear extracts of TQ-treated HEK-TLR4/MD2 cells also contain the specific active form of NFκB DNA binding activity (Fig. 1b). Anti-NFκBp65 antibodies block NFκB binding to the oligonucleotide during the reaction, reconfirming the specificity of the NFκB binding reaction (Fig. 1b). To further support the EMSA results, we also performed western blots to detect phosphorylated NFκB (pS529) in nuclear cell extracts from untreated and TQ-stimulated HEK-TLR4/MD2 cells at different time intervals. Optimal activation of NF-κB requires phosphorylation in the transactivation domain of p65. This transactivation domain of p65 subunit is responsible for the interaction with the inhibitor IkB and contains the phosphorylation sites. A phospho-specific polyclonal antibody against the human NFκBp65 pS529 (pNFκB) was used here which has minimal reactivity with non-phosphorylated p65. This phospho-specific antibody reacts with a peptide sequence (PNGLLpSGDEDFC) corresponding to a region near phospho-serine 529 of the human NFκBp65 (Rel A) protein. As shown in Fig. 1b, TQ stimulation of the cells increased NFκB pS529 in the nuclear extracts at 5, 10 and 30 min of treatment compared to the media control (time zero) and to β-actin as an internal protein control. In Fig. 1b, it is noteworthy at 15 min of treatment that TQ-induced NFκB pS529 expression in the nuclear extracts was found to decrease slightly compared to the other stimulation time intervals. These results are consistent with the EMSA findings for these same cells, suggesting that TQ-induces NFκB activation in a biphasic manner.

Western blots were also performed to detect phosphorylated NFκB (pS529) in cell lysates from Tamiflu pre-treated and TQ-stimulated HEK-TLR4/MD2 cells and untreated media control cells. As shown in Fig. 1c, Tamiflu inhibited TQ-induced NFκB pS529 in these cells compared to β-actin as an internal protein control. These latter data signify that Tamiflu may have a direct effect on the Neu4

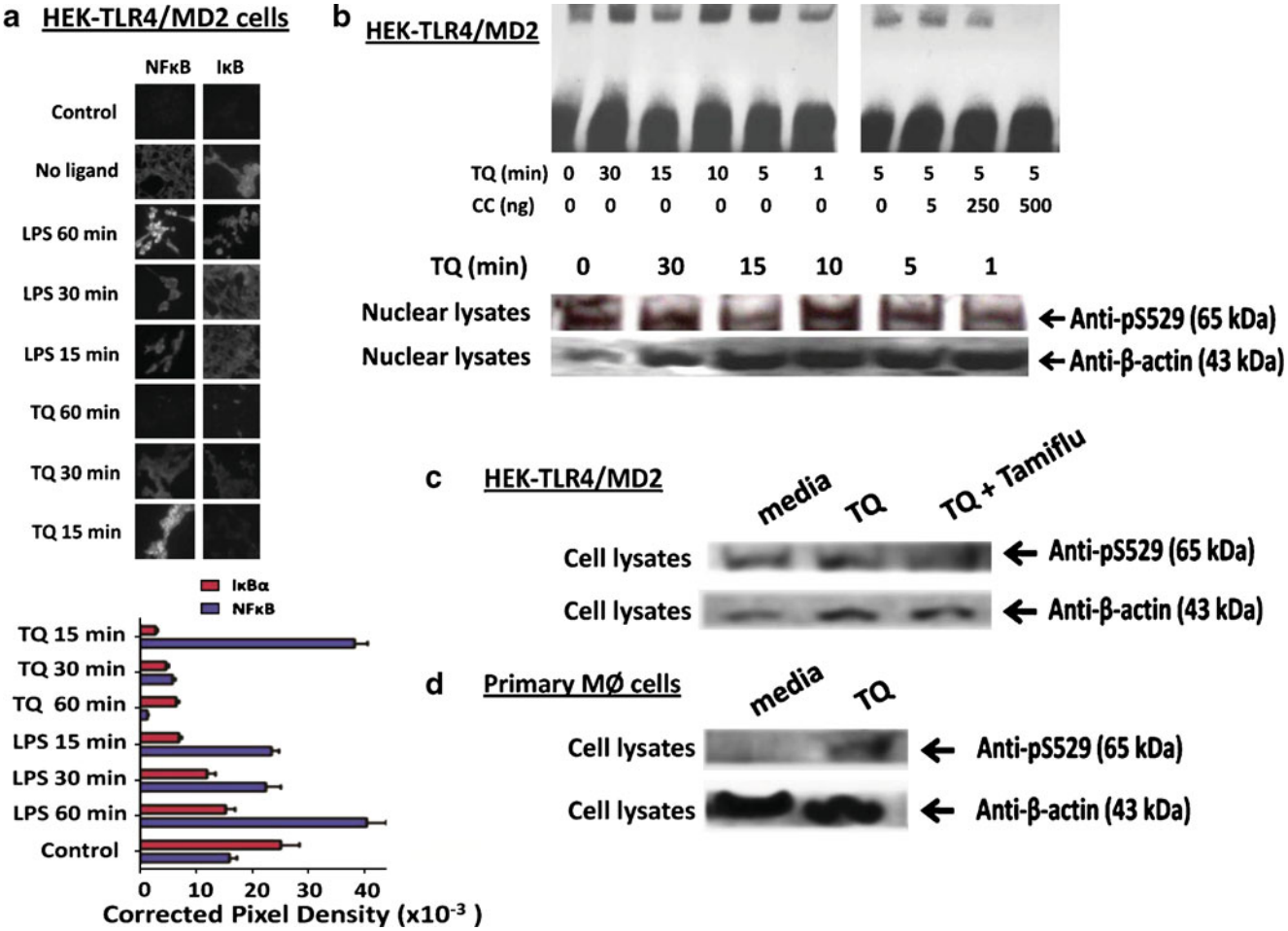

Fig. 1 TQ induces phosphorylated NFκBp65 pS529 in HEK-TLR4/MD2 cells and primary BM macrophages, which is blocked by neuraminidase inhibitor Tamiflu. **a** HEK-TLR4/MD2 cells were treated with either 5 μg/mL LPS for 15, 30 and 60 min, 100 μg/mL TQ for 15, 30 and 60 min or left untreated as no ligand control. Cells were fixed, permeabilized, and immunostained with rabbit anti-NFkBp65 or rabbit anti-IkBα followed with Alexa Fluor594 goat anti-rabbit IgG. The control group represents untreated cells immunostained with only the secondary Alexa Fluor594 goat anti-rabbit IgG. Immunostained cells were visualized by epi-fluorescence microscopy using a 40× objective. Approximately 90% of LPS- or TQ-treated cells immunostained with anti-NFkBp65 antibody had nuclear staining. Quantitative analysis was done by assessing the density of cell staining corrected for background in each panel using Corel Photo Paint 8.0 software. Each bar in the figures represents the mean corrected density of staining±SEM for all cells within the respective images. The data are a representation of one out of five independent experiments showing similar results. **b Electrophoretic mobility shift assay (EMSA)**. Supernatants containing the nuclear extracts from TQ-treated HEK-TLR4/MD2 cells at indicated times were analyzed by EMSA to detect NF-κB DNA binding activity using a 3′ biotinylated double-stranded oligonucleotide (oligo) sequence 5′ AGT TGA GGG GAC TTT CCC AGG C 3′ against the NF-κB binding site. Non-biotinylated oligo probe was used as a NF-κB binding competitor (CC). The blot was probed with Streptavidin-HRP followed with Western Lighting Chemiluminescence (PerkinElmer Life Sciences, Boston). The data are a representation of one out of four independent experiments showing similar results. **Western blot analyses of phosphorylated NFkB (pS529) in nuclear lysates**. HEK-TLR4/MD2 cells were treated with TQ as described in (B) above. Nuclear lysates from the cells were separated by SDS–PAGE and probed with phospho-specific polyclonal rabbit antibody against the human NFκBp65 pS529 with minimal reactivity with non-phosphorylated p65. β-actin was used as an internal protein control. The data are a representation of one out of three independent experiments showing similar results. **c Western blot analyses of phosphorylated NFkB (pS529) in cell lysates**. HEK-TLR4/MD2 cells were pretreated with 100 μM Tamiflu for 30 min followed with 100 μg/mL TQ for 30 min or left untreated as media control. Cell lysates from the cells were separated by SDS-PAGE and probed with polyclonal rabbit anti-NFκBp65pS529 antibody. β-actin was used as an internal protein control. The data are a representation of one out of three independent experiments showing similar results. **d Western blot analyses of phosphorylated NFkB (pS529) in cell lysates from primary BM macrophages**. Primary BM macrophages derived from WT mice were treated with 100 μg/mL of TQ for 30 min or left untreated as media control. Cell lysates from the cells were separated by SDS-PAGE and probed with polyclonal rabbit anti-NFκBp65pS529 antibody. β-actin was used as an internal protein control. The data are a representation of one out of three independent experiments showing similar results

sialidase associated with TQ treated cells. These results are consistent with our other reports indicating that Tamiflu is not only a potent inhibitor (IC_{50} of 0.0194 μM) of Neu4 sialidase associated with TQ treated live BMC-2 macrophage cells [3] but also a potent inhibitor (IC_{50} of 1.2 μM) of Neu1 sialidase associated with TLR ligand treated live macrophage cells [1]. Tamiflu was also reported to partially inhibit LPS-induced NFκB pS529 in primary macrophage cells but had no inhibitory effect on NFκB pS529 activation when the cells were treated with phorbol 12-myristate 13-acetate (PMA), a protein kinase C (PKC) activator [2].

We also examined TQ-induced phosphorylated NFκB (pS529) in primary mouse bone marrow (BM) macrophages derived from wild-type mice. Western blot analyses show NFκB pS529 activation in cell lysates from TQ-treated primary BM macrophage cells compared to untreated media control cells and to β-actin as an internal protein control (Fig. 1d).

GPCR Gαi-sensitive pertussis toxin and broad range MMP inhibitor galardin completely inhibit TQ-induced NFκB activation in BMC-2 macrophage cells and HEK-TLR4/MD2 cells, and MyD88/TLR4 complex formation in primary BM macrophages

In a recent report, we showed that GPCR Gαi-sensitive pertussis toxin (PTX) and the broad range inhibitors of matrix metalloproteinase (MMP) galardin and piperazine applied to live BMC-2 macrophage cells, human monocytic THP-1 cells and primary BM macrophage cells completely block TQ-induced sialidase activity [3]. These same inhibitory effects were not observed with the GM1 ganglioside specific cholera toxin subunit B (CTXB) as well as with CTX, tyrosine kinase inhibitor K252a, and the broad range GPCR inhibitor suramin [3]. Here, we hypothesize that PTX and galardin would inhibit TQ-induced NFκB activation in BMC-2 macrophage and HEK-TLR4/MD2 cells. The data in Fig. 2a and b support this hypothesis. Galardin (GM6001), a broad specific inhibitor of MMP-1, −2, −3, −8 and −9, and pertussis toxin (PTX), a specific inhibitor of G_{i2} and G_{i3} (α subunits) of G protein subtypes as well as Tamiflu completely blocked TQ-induced NFκB activation in BMC-2 cells (Fig. 2a). To confirm these results, western blot analyses of nuclear extracts from HEK-TLR4/MD2 cells pretreated with these same inhibitors followed with TQ-stimulation clearly show complete blockage of NFκB pS529 activation compared to TQ-treated positive controls and β-actin as an internal protein control (Fig. 2b).

If TQ-induced NFκBpS529 activation is blocked by Tamiflu, pertussis toxin and galardin, we also predicted that these same inhibitors would inhibit TQ-induced MyD88/TLR4 complex formation in primary BM macrophage cells. The data in Fig. 2c show this to be the case. Using confocal microscopy to detect MyD88 colocalization with TLR4, there was a significant reduction of TQ-induced MyD88/TLR4 complex formation in primary BM macrophages pretreated with Tamiflu (9.2% overlay), galardin (13.8% overlay) and pertussis toxin (PTX) (1.3% overlay) compared to the TQ-treated positive control (35.6% overlay). In addition, the TQ-induced MyD88/TLR4 complex formation in these primary cells was comparable to the LPS-treated (46.2% overlay) cells.

It is noteworthy here that BMA macrophage cells pretreated with Tamiflu, pertussis toxin and galardin for 30 min and followed by TQ stimulation for another 30 min as in Fig. 2a and c had no effect on cell viability (Fig. 2d).

To confirm that Neu4 sialidase is primarily involved with TQ-induced MyD88/TLR4 complex formation, we also examined this in primary mouse BM macrophages derived from Neu4-knockout mice. Using confocal microscopy to detect MyD88 colocalization with TLR4, the data in Fig. 3a clearly indicate a lack of MyD88/TLR4 complex formation (0% overlay) in primary macrophage cells from Neu4 knockout mice in comparison to the same cells treated with TLR4-ligand lipopolysaccharide (LPS, 5 μg/mL) (31% overlay) and TLR2-ligand killed *Mycobacterium butyricum* (Myco, 5 μg/mL) (35% overlay). In contrast, TQ induced MyD88/TLR4 complex formation in primary macrophages from WT and Neu1-deficient mice. These latter data with the Neu1-deficient macrophages are consistent with other reports showing that Neu4 can target substrates of Neu1 sialidase and restore normal morphological phenotype of the lysosomal compartment in Neu1-deficient sialidosis fibroblasts [15].

Neu4 forms a complex with MMP9 and circuitously targets TLR4 receptors already bound with MMP9

We recently reported that Neu4 in alliance with GPCR-signaling Gαi subunit proteins and MMP-9 is expressed on the cell surface of human monocytic THP-1 cells, human WT and WG0544 sialidosis type I fibroblast cells and BMC-2 macrophage cells [3]. This tripartite alliance made Neu4 readily available to be induced by TQ. Indeed, Neu4 sialidase activity in TQ-treated live cells occurred within a minute. Since Neu4 does not form a complex with TLR4 receptors [1], we questioned whether there is an intermediate link between this Neu4 tripartite alliance and TLR4 receptors. To test this hypothesis, we performed co-immunoprecipitation experiments using HEK-TLR4/MD2 and BMC-2 macrophage cells. The data shown in Fig. 3b validated the predicted association of Neu4 with MMP-9. As predicted, MMP-9 co-immunoprecipitated with Neu4, and conversely Neu4 co-immunoprecipitated with MMP-9 in cell lysates from naïve HEK-TLR4/MD2 cells. In addition, MMP-9 co-immunoprecipitated with TLR4 receptors, and conversely TLR4 co-immunoprecipitated with MMP-9 in cell lysates from naïve BMC-2 cells (Fig. 3c). These latter data further

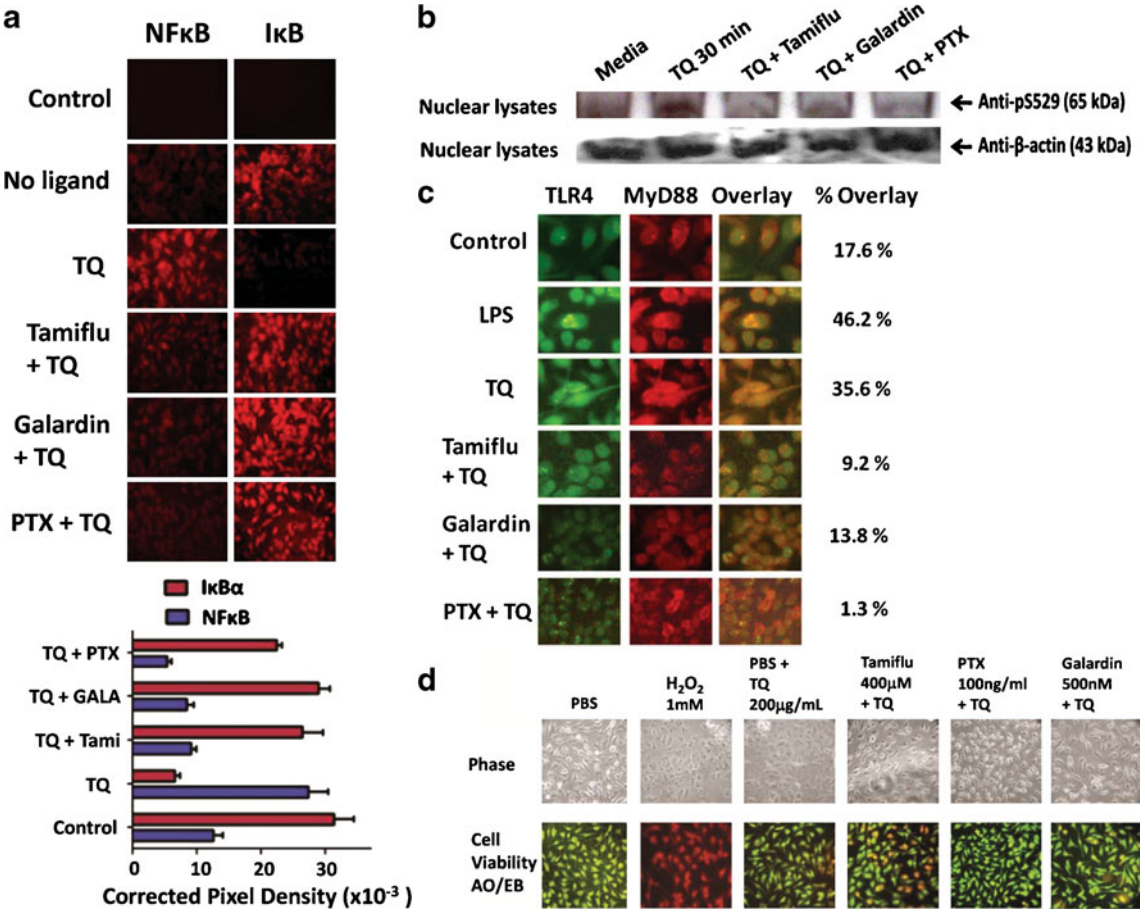

Fig. 2 a Tamiflu, MMP inhibitor galardin and Gαi-sensitive pertussis toxin inhibited TQ-induced NFκB activation in BMC-2 macrophage cells. Cells were grown on 12 mm circular glass slides in DMEM medium containing 5% fetal calf serum for 48 h at 37°C. After removal of medium, cells were left untreated as no ligand control or pretreated with 200 μM Tamiflu, 500nM Galardin, or 100 ng/ml pertussis toxin (PTX) for 30 min followed with 200 μg/mL TQ for 30 min. Cells were fixed, permeabilized and immunostained with rabbit anti-NFkBp65 or rabbit anti-IkBα followed with Alexa Fluor594 goat anti-rabbit IgG. The control group represents untreated cells immunostained with only the secondary Alexa Fluor594 goat anti-rabbit IgG. Immunostained cells were visualized by epi-fluorescence microscopy using a 40× objective. Approximately 90% of LPS- or TQ-treated cells immunostained with anti-NFkBp65 antibody had nuclear staining. These data are representative of one of three individual experiments. **b Western blot analyses of phosphorylated NFkB (pS529) in nuclear lysates**. Nuclear extracts were obtained from the HEK-TLR4/MD2 cells pretreated with 200 μM Tamiflu, 500nM Galardin or 100 ng/ml pertussis toxin (PTX) for 30 min followed with 100 μg/mL TQ for 30 min. Nuclear lysates from the cells were separated by SDS-PAGE and probed with anti-NFκBp65 pS529 antibody. β-actin was used as an internal protein control. The data are a representation of one out of two independent experiments showing similar results. **c Tamiflu, galardin and pertussis toxin inhibit TQ-induced MyD88 co-localization with TLR4 in primary BM macrophage cells derived from wild-type mice**. Primary macrophages were grown on 12 mm circular glass slides in DMEM medium containing 10% fetal calf serum, 20% monocyte colony stimulating factor (M-CSF) and 1× L-glutamine-penicillin-streptomycin (Pen-Strep) for 8 days at 37°C. After removal of medium, cells were treated with 5 μg/ml lipopolysaccharide (LPS), 100 μg/mL TQ or 100 μg/mL TQ in combination with 200 μM Tamiflu, 500 nM Galardin or 100 ng/mL pertussis toxin (PTX) for 5 min. Cells were fixed, permeabilized and immunostained with rabbit anti-mouse anti-MyD88 and rat anti-mouse anti-TLR4 for 60 min. Cells were washed and stained with goat anti-rabbit AlexaFluor 594 for 60 min and rabbit anti-rat AlexaFluor 488 for 60 min. Fluorescent images were taken by confocal microscopy using a 40× objective. These data are representative of two individual experiments. **d Cell Viability in BMA macrophage cells treated with Tamiflu, galardin and pertussis toxin in the presence of TQ**. Cells were grown on 12 mm circular glass slides in medium containing 5% fetal calf serum and 100 μg/mL G418 for 24 h at 37°C in 5% CO_2. The medium was removed and the cells were left alone (control), or treated with Tamiflu, galardin and pertussis toxin in the presence of TQ as described in (A,C above) or with 1 mM hydrogen peroxide (H_2O_2) for 30 min. Cell viability was assessed by acridine orange/ethidium bromide (AO/EB) staining and epi-fluorescence microscopy. The data represent one of two independent experiments showing similar results

validated that MMP-9 forms a complex with naïve TLR4 receptors on the cell surface. Taken together, these results indicate that MMP-9 in complex with TLR4 is the intermediate link for TQ-induced Neu4 circuitously targeting TLR4 receptors, and enabling removal of steric hinderance for receptor association.

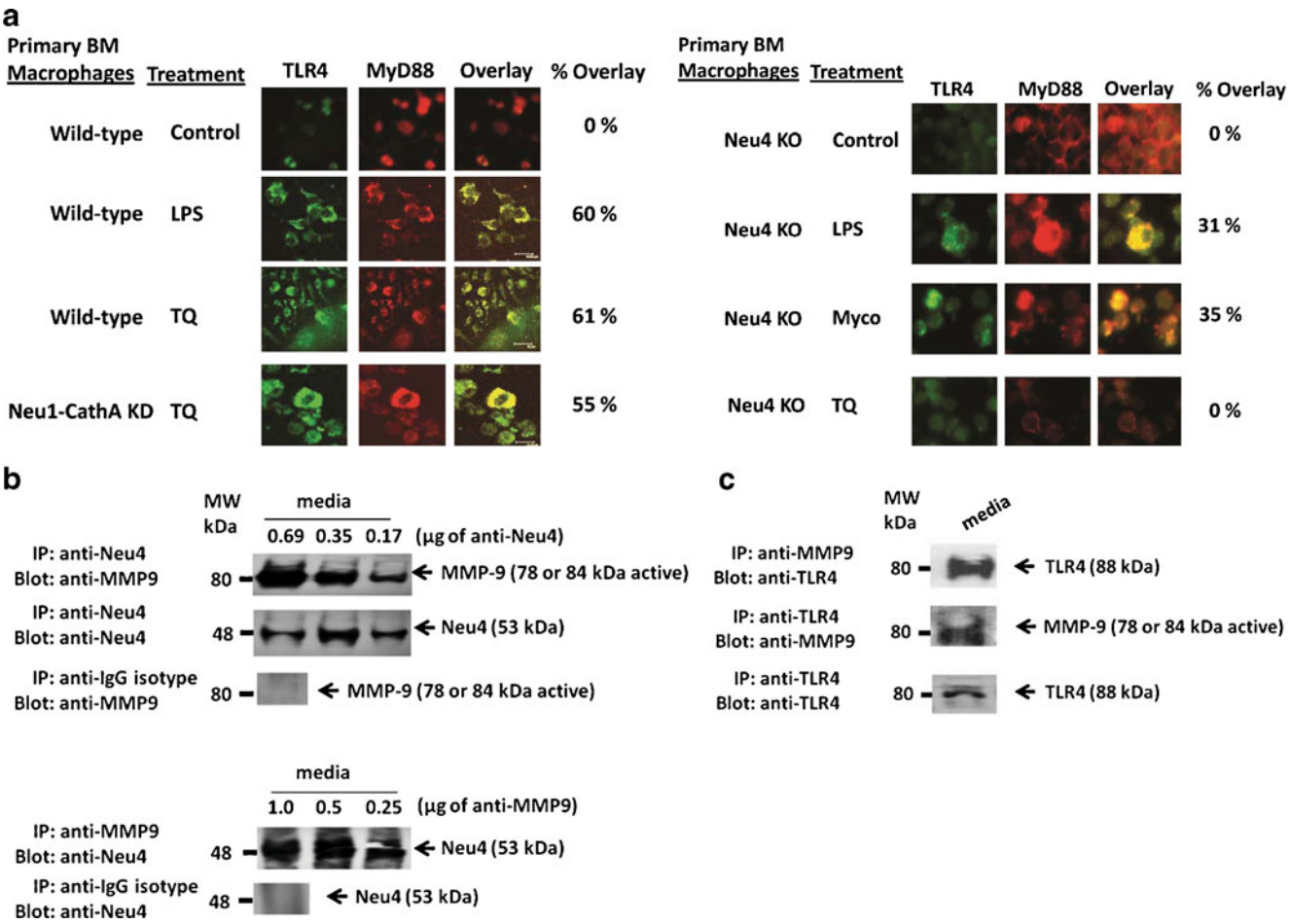

Fig. 3 a TQ-induced colocalization of MyD88 and TLR4 in primary bone marrow (BM) macrophage cells. Primary BM macrophage cells obtained from wild-type, Neu1-CathA KD (Neu1 deficient and cathepsin A deficient) and Neu4 KO (Neu4 knockout) mice were cultured in medium supplemented with 20% (v/v) monocyte-colony stimulating factor (M-CSF), 10% FCS and Penn/Strep/Glut for 8 days on circular glass slides in 24 well tissue culture plates as described previously [14]. Cells were stimulated with either 3 µg/mL LPS, 5 µg/mL killed *Mycobacteria butyricum* (Myco) or 100 µg/mL TQ for 5 min or left untreated (no ligand control). Cells were fixed, permeabilized and immunostained with rabbit anti-mouse anti-MyD88 and rat anti-mouse anti-TLR4 for 60 min. Cells were washed and stained with goat anti-rabbit AlexaFluor 594 for 60 min and rabbit anti-rat AlexaFluor 488 for 60 min. Stained cells were visualized using a confocal inverted microscope (Leica TCS SP2 MP inverted Confocal Microscope) with a 100× objective (oil). Images were captured and processed using Image J 1.38× software (NIH, USA). To calculate the amount of colocalization in the selected images, the Pearson correlation coefficient was measured and expressed as a percentage using Image J 1.38× software. The data are a representation of two independent experiments showing similar results. **b Co-immunoprecipitation and Western blot analyses of Neu4 and MMP9**. HEK-TLR4/MD2 cells were left untreated as media control. Cells were pelleted, lysed in lysis buffer and the protein lysates were immunoprecipitated with indicated µg of anti-Neu4 or anti-MMP9 for 24 h. The same protein lysates were immunoprecipitated with anti-IgG isotype control antibodies. Immunocomplexes were isolated using protein A or G magnetic beads, resolved by SDS-PAGE and the blot probed with the indicated primary antibodies followed with Clean-Blot IP Detection Reagent. The data are a representation of one out of three independent experiments showing similar results. **c Co-immunoprecipitation and Western blot analyses of MMP9 and TLR4**. BMC-2 macrophage cells were left untreated as media control. Cells were pelleted, lysed in lysis buffer and the protein lysates were immunoprecipitated with anti-MMP9 or anti-TLR4 antibodies for 24 h. Immunocomplexes were isolated using protein A or G magnetic beads, resolved by SDS-PAGE and the blot probed with the indicated primary antibodies followed with Clean-Blot IP Detection Reagent. The data are a representation of one out of four independent experiments showing similar results

Neu4 sialidase activation associated with TQ treated live cells is not due to an increased Neu4 protein expression on the cell surface with time

It is interesting to note from our previous report that there was no correlation between mRNA and protein values for Neu3 and Neu4 in human monocytic THP-1 cells [3]. The RT PCR data showed that in naïve THP-1 cells, the Neu3-specific RNA values were relatively high in comparison to the expression of β-actin as an internal control while Neu4-specfic RNA values were absent. However, western blot analyses of the cell lysates revealed that the Neu3 and Neu4 protein profiles did not correlate with the mRNA values. The results revealed high Neu4 protein values and very low Neu3 protein expression

even though immunoprecipitation of Neu3 in the cell lysates revealed Neu3 presence. Collectively, these findings provided for the first time a varied post-transcriptional mechanism for these two mammalian sialidases even when they have similar functions [3]. Since Neu4 is expressed on the cell surface of naïve THP-1 cells as well as on WT and sialidosis type 1 fibroblast cells [3], we asked whether the Neu4 sialidase activity associated with TQ treated live CD14-THP-1 cells is attributed to increased Neu4 protein expression on the cell surface or increased sialidase activity with time.

To test the latter hypothesis, we measured TQ-induced sialidase activity in the cell suspensions of CD14-THP1 cells using a Varioskan fluorescence spectrophotometer. To 50 μL of cell suspension (0.5×10^6 cells/mL or 1.0×10^6 cells/mL) from 90% cell confluence in 25-cm^2 flasks of serum-free medium, 100 μg/mL TQ and 0.318 mM 4-MUNANA substrate were added to MicroFluor black microtiter plates at different time intervals or were left untreated as controls. The fluorescence intensity readings were immediately taken over 4 min using fluorescence emission at 450 nm and an excitation at 365 nm. The data clearly show TQ-induced sialidase activity in live CD14-THP1 cells. This activity was cell density dependent (Fig. 4a) but decreased after 2 min and remained at a constant level over 4 min. The sialidase activity in each of the cell samples was calculated from a standard sialidase activity curve (Fig. 4a) and expressed as milli Units (mU) per mg of 4-MUNANA for each of the time intervals.

To test for Neu4 protein levels on the cell surface, CD14-THP-1 cells were stimulated with TQ for 5, 10, 15 and 30 min or left untreated as controls. The immunolocalization of Neu4 together with TLR4 and MMP9 on the cell surface of these cells was confirmed by flow cytometry using live cells immunostained with either PerCP/Cy5.5 conjugated anti-Neu4 antibodies (Fig. 4b), fluorescein conjugated anti-TLR4 antibody (Fig. 4c) or anti-MMP9 primary antibody followed with Alexa fluor 488 conjugated secondary antibody (Fig. 4d). The data shown here clearly indicate that 15,000 acquired live, untreated and TQ-stimulated CD14-THP1 cells over the indicated time intervals showed significant immunostaining for Neu4 and TLR4 expressions on the cell surface. These data provide clear evidence to support Neu4 stability on the cell surface after TQ treatment over 30 min. It is interesting to note that there was a significant diminution of MMP9 protein expression on the cell surface at 15 min of TQ treatment but it rebounded to media control levels at 30 min. These latter data appear to coincide with the biphasic response of TQ-induced pNFκB activation at 15 min.

Physiological relevance of Neu4 sialidase in regulating TQ-induced pro-inflammatory cytokines

If TQ-induced Neu4 sialidase activity is associated with TLR4 receptors in live macrophage cells, we also asked if TQ-induced Neu4 has a physiological relevance in regulating pro-inflammatory cytokines. Cytokine analyses were performed to determine if mice treated with TQ were able to produce pro-inflammatory responses. Cytokine profile arrays of 40 different cytokines and chemokines were executed on the serum extracted from wild-type, Neu1 deficient and Neu4 knock-out (Neu4KO) mice before and 5 h after an intraperitoneal injection of 2 mg/kg of TQ. Serum was incubated with pre-labeled membranes containing the antibodies for 40 different cytokines as described in the R&D System Cytokine Array Profiling ARY066 kit (R&D Systems, Inc., Minneapolis). The data in Figs. 5 and 6 indicate that WT and Neu1-deficient mice had an increase in the levels of most cytokines after treatment with TQ, while the cytokine levels in the serum from Neu4 KO mice remained the same or decreased after treatment with TQ. Several pro-inflammatory cytokines were highly expressed in the serum of the WT and Neu1-deficient mice after treatment with TQ including sICAM-1, IFN-γ, IL-1α, IL-1β, IL-6, TREM-1 and TNF-α (Fig. 5). Chemokines such as CXCL1, CCL2, MIP-1α and β (CCL 3 and 4 respectively), and MIP-2 (CXCL2) also increased by 2-fold or more after TQ treatment of WT and Neu1-deficient mice (Fig. 5). WT and Neu1-deficient mice treated with TQ produced no increase in the anti-inflammatory cytokine IL-10 with little fold increase in other anti-inflammatory cytokines such as IL-4 (Fig. 6). Taken together, TQ induced pro-inflammatory cytokines and chemokines are partially dependent on Neu4 sialidase.

To further confirm TQ-induced pro-inflammatory cytokines, RT-PCR analyses were also performed on RNA extracts from untreated and TQ treated of HEK-TLR4/MD2 cells at 2, 4, 6 or 8 h. As positive controls, cells were treated with 5 μg/mL LPS for 4 h. The relative amounts of IL-6, TNF-α and MIP-1β mRNAs in naïve, untreated and TQ-treated HEK-TLR4/MD2 cells compared to RNA encoding β-actin are shown in Fig. 6b. The amount of RNA encoding IL-6, TNF-α and MIP-1β was clearly elevated after 4 h of TQ treatment in relation to the amount of mRNA for β-actin, LPS-treated positive controls and untreated control cells. There was no evidence of mRNAs for these cytokines after 6 h treatment with TQ. Taken together, the data provide evidence to support the premise that there is a definitive correlation between mRNA and cytokine values for IL-6, TNF-α and MIP-1β following TQ treatment *in vitro* and *in vivo*.

Discussion

The data presented in this report provide evidence for the first time that MMP-9 may be an important intermediate link in the TQ-induced Neu4 sialidase activity. Central to

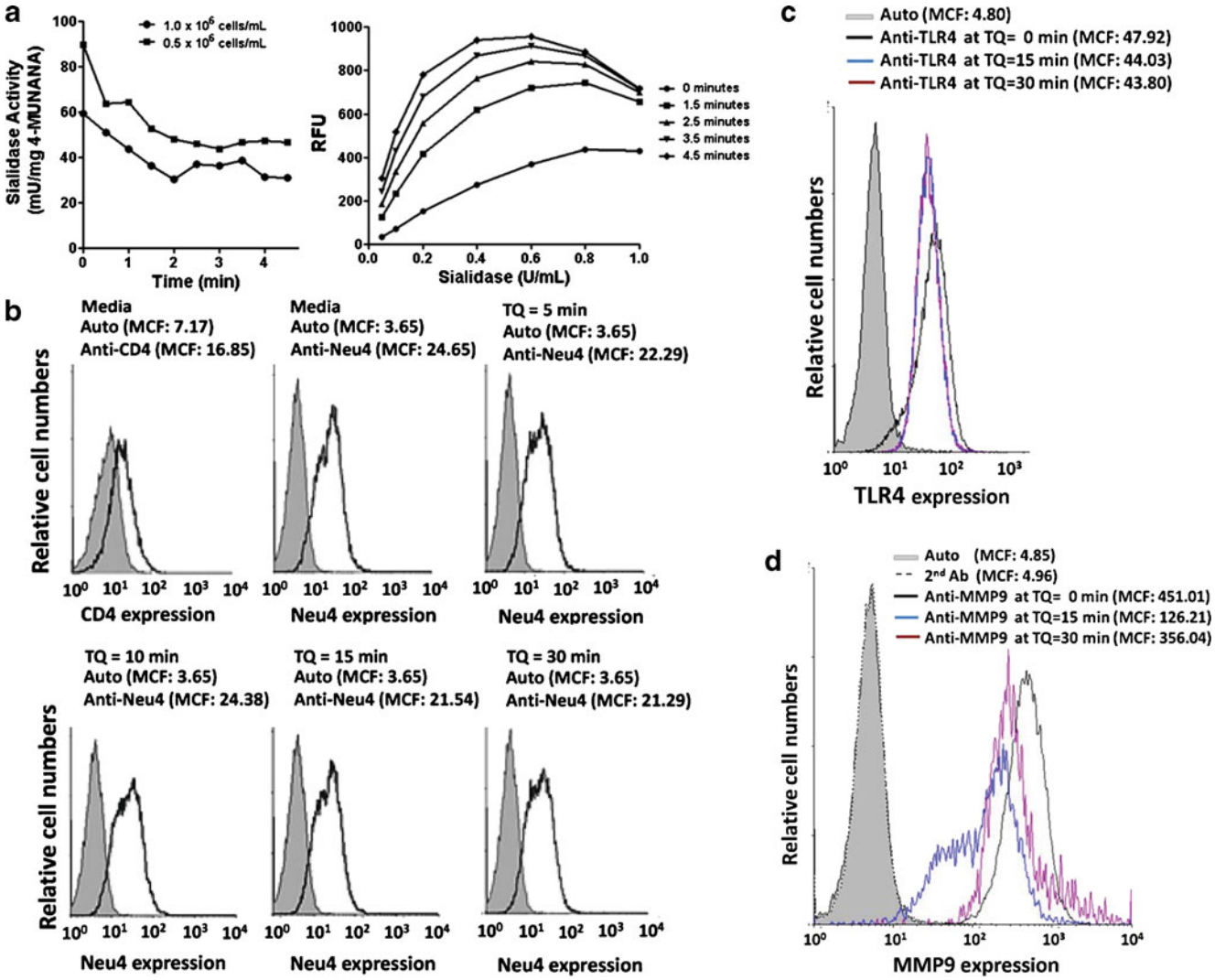

this process is that Neu4 forms a complex with MMP-9, which is already bound to TLR4 receptors. Neu4 linked to MMP9 can circuitously target TLR4 receptors. This would actually make Neu4 tethered to TLR4 receptors readily available to target sialyl residues, enabling removal of steric hinderance to receptor association. Our data support this hypothesis because TQ-induced Neu4 sialidase activity in live TLR4-expressing cells promotes MyD88/TLR4 complex formation and subsequent NFκB activation and cell function.

It is noteworthy that TQ induces NFκB activation in a biphasic manner (Fig. 1b). The data are in support of an oscillatory pattern of NFκB activation in response to many other stimuli [16]. The majority of NFκB resides in the cytoplasm, bound to the IκB inhibitory family of proteins, which include IκBα, IκBβ, IκBε, Bcl-3, p100, and p105. These proteins function as inhibitors through ankyrin repeats, which bind to the REL domain of NFκB and mask the nuclear localization signal (NLS) site in preventing NFκB nuclear translocation. Activation of NF-κB is well known to be mediated through the IκB kinase complex (IKK), which has the function to phosphorylate two serine residues on IκB proteins. The phosphorylation of these residues causes the ubiquitination and subsequent degradation of IκB proteins by the 26S proteasome complex [17]. As a consequence, NFκB NLS is uncovered and nuclear translocation occurs where it binds to its cognate DNA sequence to stimulate gene expression. One of the numerous genes induced by NF-κB is its own IκBα inhibitor [18–21]. Depending on the activating signal and cell type, IκBα inhibitor can be resynthesized. The newly synthesized IκBα is then transported to the nucleus where it binds and inhibits NF-κB DNA binding [22]. NF-κB is then sequestered back to the cytoplasm through a nuclear export signal located in the amino terminus of IκBα [23]. This process would establish the signalling profile of a biphasic NF-κB activation, which is dependent on the IKK/26S proteasome pathway. Others have reported that TNFα

◀ **Fig. 4 a TQ-induced sialidase activity in cell suspensions of CD14-THP1 cells**. Cells at 90% confluence in 25-cm^2 flasks were resuspended in 5 ml of Tris-buffered saline. 50 μL of 0.5×10^6 cells/mL or 1.0×10^6 cells/mL was added to 100 μg/mL TQ and 0.318 mM 4-MUNANA substrate; the remaining cells in the presence of substrate were left untreated as controls. The fluorescence intensity readings were immediately taken over 5 min using the Varioskan Fluorescence Spectrophotometer (Type 3001, Microplate Instrumentation, Thermo Electron Corporation, Vantaa, Finland) at emission 450 nm following an excitation at 365 nm. The sialidase activity in the live cells was calculated from a standard sialidase activity curve, and expressed as milli Units per mg of 4-MUNANA after subtracting endogenous background sialidase activity in untreated cells in the presence of substrate. The average background endogenous sialidase activity in the control untreated live cells was 451.7 mU per mg 4-MUNANA taken at different time intervals. Standard sialidase activity curve at the indicated reaction times was determined using 50 μL of neuraminidase (*Clostridium perfringens*; a specific activity of 1 U per 1.0 mmole of *N*-acetylneuraminic acid per minute) at different units/mL added to 50 μL of 0.318 mM 4-MUNANA substrate. The relative fluorescence intensity readings (RFU) were immediately taken over 5 min using the Varioskan Fluorescence Spectrophotometer. **b Flow cytometry analysis of Neu4 expressed on the cell surface of live CD14-THP1 cells treated with TQ for 0–30 min**. Live cells were treated with 100 μg/mL TQ at the indicated time intervals, washed and stained for CD14 and Neu4. Histograms show staining for CD14 with fluorescein conjugated anti-CD14 antibody and for Neu4 with PerCP/Cy5.5 tandem conjugated rabbit polyclonal anti-Neu4 after incubation on ice for 30 min. Stained cells were analyzed by Beckman Coulter Epics XL-MCL flow cytometry and Expo32 ADC software (Beckman Coulter). Overlay histograms are displayed. Control unstained live cells (auto) are represented by the gray-filled histogram. Live cells stained with anti-CD14 or anti-Neu4 antibodies are depicted by the unfilled histogram with the black line. The mean channel fluorescence (MCF) for each histogram is indicated for 15,000 acquired cells (50% gated). The data are a representation of one out of three experiments showing similar results. **c Flow cytometry analysis of TLR4 expressed on the cell surface of live CD14-THP1 cells treated with TQ for 0, 15 and 30 min**. Live cells were treated with 100 μg/mL TQ at the indicated time intervals, washed and stained for TLR4. Histograms depict staining for TLR4 with fluorescein conjugated anti-TLR4 antibody after incubation on ice for 30 min. Stained cells were analyzed as described in (**b**). Non-stained live cells (auto) are represented by the gray-filled histogram. Live cells stained with anti-TLR4 antibodies are depicted by the unfilled histogram with the black line (0 min TQ untreated), blue line (15 min TQ treatment) and purple line (30 min TQ treatment). The mean channel fluorescence (MCF) for each histogram is indicated for 15,000 acquired cells (50% gated). The data are a representation of one out of three experiments showing similar results. **d Flow cytometry analysis of MMP9 expressed on the cell surface of live CD14-THP1 cells treated with TQ for 0, 15 and 30 min**. Live cells were treated with 100 μg/mL TQ at the indicated time intervals, washed and stained for MMP9. Histograms depict staining for MMP9 with rabbit polyclonal anti-MMP9 antibody after incubation on ice for 30 min followed with AlexaFluor 488 conjugated F(ab')$_2$ secondary antibody for 30 min. Stained cells were analyzed as described in (**b**). Non-stained live cells (auto) are represented by the gray-filled histogram. Live cells stained only with AlexaFluor 488 conjugated F(ab')$_2$ secondary antibody are depicted by the unfilled histogram with the dashed line. Live cells stained with anti-MMP9 antibodies and AlexaFluor 488 conjugated F(ab')$_2$ secondary antibody are depicted by the unfilled histogram with the black line (0 min TQ untreated), blue line (15 min TQ treatment) and purple line (30 min TQ treatment). The mean channel fluorescence (MCF) for each histogram is indicated for 15,000 acquired cells (50% gated). The data are a representation of one out of three experiments showing similar results

induces NFκB activation in a biphasic manner [16]. They have shown that the regulation of the first transient phase is mediated by the degradation and subsequent resynthesis of IκBα, as well as by a TNFα-induced expression of a tumor necrosis factor (TNF)-inducible NFkB-regulated zinc finger protein (A20). The second phase activity correlates with the persistent down-regulation of both IκBα and IκBβ proteins, derived from a continuous TNFα signal. In our studies, the TQ-induced biphasic NFκB activation appears to follow the similar signalling profile of the TNF pattern.

With regard to TLR receptors, we have shown that Neu4 does not form a complex with TLR-2, −3 and −4 receptors [1]. However, we did report an unprecedented membrane controlling mechanism that is initiated by ligand binding to TLR-2, −3 and −4 to induce Neu1 sialidase activity within minutes in live primary bone marrow (BM) macrophage cells and macrophage and dendritic cell lines [1]. The premise is that Neu1 and not the other mammalian sialidases Neu2, −3 and −4 forms a complex with TLR-2, −3 and −4 on the cell surface of naïve macrophage cell lines. Endotoxin LPS binding to TLR4 induces Neu1 with subsequent activation of NFκB and the production of nitric oxide and pro-inflammatory IL-6 and TNFα cytokines in primary and macrophage cell lines [1]. The mechanism of TLR receptor activation by ligand binding to its respective receptors was found to be dependent on the removal of α2-3 sialyl residues linked to β-galactoside of TLR4 by the Neu1 activity associated with LPS-stimulated live primary macrophage cells, macrophage and dendritic cell lines but not with primary Neu1-deficient macrophage cells [2]. Since Neu1 and Neu4 mammalian sialidases have similar substrate specificities [15], it would be most likely that Neu4 also targets α2-3 sialyl residue(s) linked to β-galactoside of TLR4. Since Neu4 does not form a complex with TLR4 receptors like Neu1 [1], the data in this report supports an unprecedented molecular signaling platform involving MMP9 bound to TLR4 as the intermediary linker for Neu4 in targeting α2-3 sialyl residue(s) linked to β-galactoside residues of TLR4 receptors.

For the first time, we also reported a novel activation of Neu4 sialidase on the cell surface of live macrophage, dendritic, and fibroblast cells by thymoquinone derived from the extract of *Nigella sativa* black seed (cumin) oil [3]. The findings also provided evidence for the potentiation of GPCR-signaling via membrane targeting of Gαi subunit proteins and matrix metalloproteinase-9 activation in inducing Neu4 sialidase by TQ on the cell surface. Central to this process is that Neu4 in alliance with GPCR-

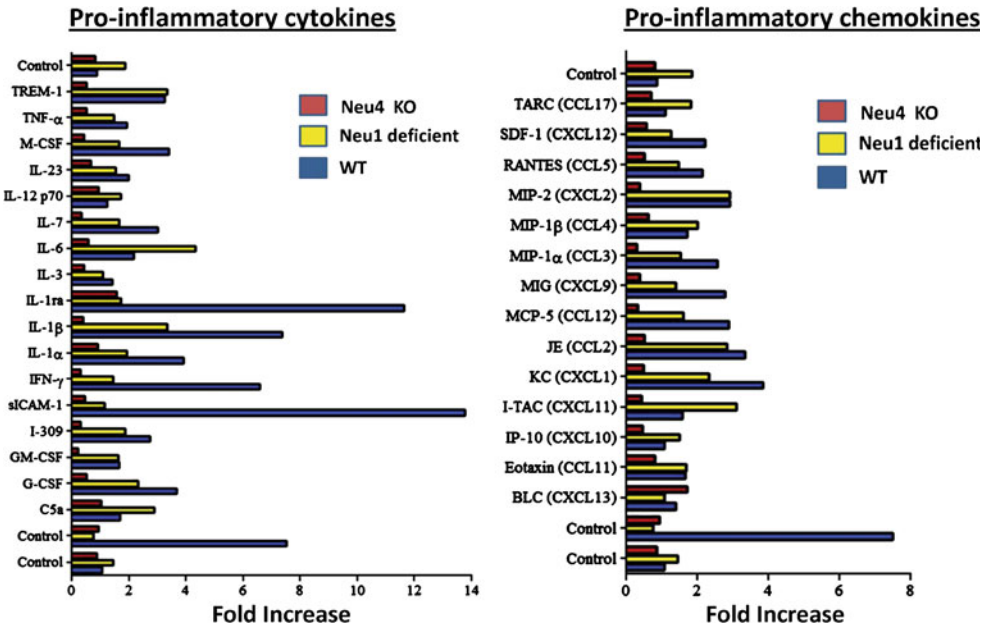

Fig. 5 *In vivo* **TQ induced serum cytokine production in wild-type (WT), Neu1-deficient (Neu1 deficient and cathepsin A deficient) and Neu4 KO (Neu4 knockout) mice**. Five mice in each group were bled before (no TQ) and 5 h after i.p. injection with 2 mg/kg of TQ per mouse. Serum was extracted from blood and immediately analyzed for cytokine and chemokine array profiling with R&D System Cytokine Array Profiling kit. The serum was mixed with the antibody detection cocktail for 1 h at room temperature followed by an overnight incubation with the membranes at 4°C. Membranes were then incubated with streptavidin-HRP for 30 min at room temperature. Quantitative analysis was done by assessing the density of spot staining corrected for background in each panel image using Pierce chemiluminescent detection reagents and Fluorchem HD2 Imaging System. The histograms depict fold increase by dividing the pixel density after TQ treatment by the pixel density of the untreated sample of the same mouse. Fold increases of greater than one represent an increase in cytokine production after treatment with TQ whereas fold values less than one represent a decrease in cytokine production after treatment. The controls depicted in each of the images are the three positive control spot signals used to identify the spot array signals in the developed film by placing the kit's transparency overlay on the array image and aligning it with the three pairs of positive control spots in the corners of each array. These data represent one of eight individual experiments showing similar results

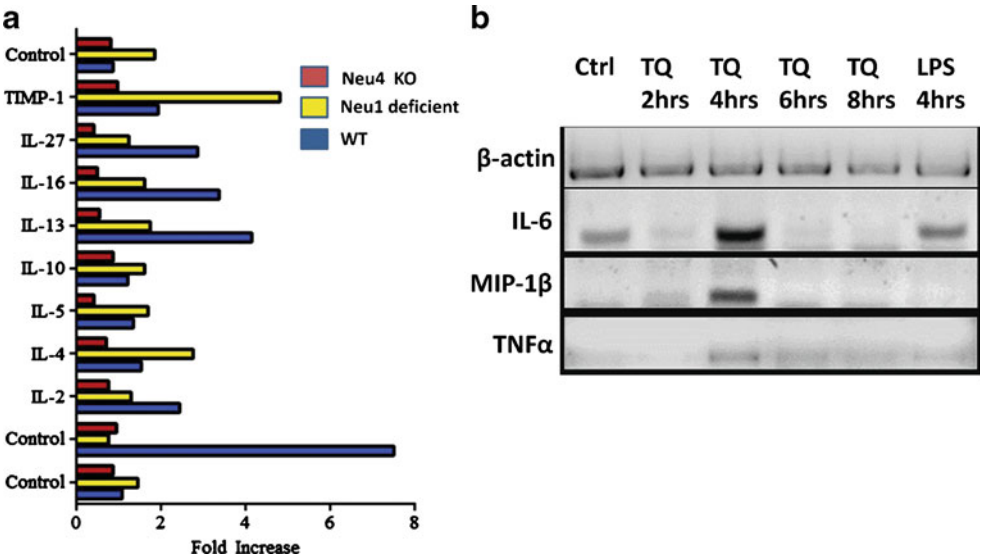

Fig. 6 **a** Sera from the same TQ treated mice as described in Fig 5 were analyzed for other cytokines with cytokine and chemokine array profiling using the R&D System Cytokine Array Profiling kit and analyzed similarly. **b Expression of RNA-specific IL-6, MIP-1β and TNFα in naïve and TQ- and LPS-treated HEK-TLR4/MD2 cells**. Cells were cultured in medium or in the presence of 100 μg/mL of TQ for 2, 4, 6, or 8 h, or with LPS for 4 h as a positive control. The indicated cytokine mRNAs were evaluated by RT-PCR analysis using total RNAs from naïve and TQ- and LPS-treated cells. Amplification of β-actin mRNA served as an internal control for RNA loading. Samples were run on a 1.2% agarose gel containing ethidium bromide. Bands were visualized using Fluorchem HD2 Imaging System. The data are a presentation of one out of three independent experiments showing similar results

signaling Gαi subunit proteins and MMP-9 is expressed on the cell surface of human monocytic THP-1 cells, human WT and WG0544 sialidosis type I fibroblast cells and BMC-2 macrophage cells. How Neu4 sialidase is rapidly induced by MMP-9 together with GPCR Gαi subunit proteins remains unknown. We would predict that TQ may target a putative cell surface Gαi-sensitive pertussis toxin GPCR as previously described [3]. The findings in this report are consistent with this prediction. Pertussis toxin and the MMP inhibitor galardin completely inhibit TQ-induced MyD88/TLR4 complex formation and subsequent NFκB activation in HEK-TLR4/MD2 cells and primary BM macrophages. According to other reports, agonist-bound GPCRs have been shown to activate numerous MMPs [4], including MMP-3 [5], MMPs 2 and 9 [6, 7], as well as members of the ADAM family of metalloproteases: ADAM10, ADAM15 and ADAM17 [8, 9].

Using flow cytometry analyses, we have also shown that both Neu4 and MMP-9 are expressed on the cell surface of live macrophage and fibroblast cells [3]. Also, Neu4 was found to be expressed on the cell surface of human sialidosis type I fibroblast cells, which are genetically deficient in Neu1, and predictably TQ was found to induce Neu4 sialidase activity in these live sialidosis type I fibroblast cells. Seyrantepe *et al*. have shown that Neu4 can completely eliminate undigested substrates of Neu1 and restore normal morphological phenotype of the lysosomal compartment in these Neu1-deficient sialidosis fibroblasts [15]. For Neu4 expression on the cell surface, our findings are surprising in lieu of the fact that primary structural analyses of Neu4 rules out the possibility of it being a transmembrane protein [24]. Thus, the subcellular distribution of the short and long forms of Neu4 [25] and their membrane anchoring mechanism still remains to be determined. Using protein extraction and cross-linking experiments, Bigi *et al*. demonstrated that both forms of Neu4 are actually extrinsic membrane proteins, anchored via protein-protein interactions [24]. Confocal microscopy and subcellular fractionation experiments have revealed that the long form localizes in the mitochondria bound to the outer mitochondrial membrane, while the short form is associated with the endoplasmic reticulum [24]. In addition, we provided evidence to indicate that Neu4 is an extrinsic cell surface membrane protein, and the data in this and our previous report [3] suggest that Neu4 may be anchored there via its interaction with matrix metalloproteinase-9. In this present report, the expression of Neu4 and TLR4 was found to be stable on the cell surface over 30 min of TQ treatment, suggesting that the observed TQ-induced sialidase activity is not due to the Neu4 enzyme being released in the extracellular environment. In addition, we have shown using a newly developed sialidase assay [1–3, 26] that live cells treated with the substrate alone did not show any fluorescence surrounding the cells [3]. Instead, they revealed an internal blue fluorescence indicating substrate internalization by the cell suggesting the catabolism of the fluorescent substrate can occur intracellularly. However, when the cells were treated with TQ together with the substrate, the sialidase activity as revealed by a fluorescence (λem 450 nm) surrounding the cells was variable from being largely cell associated to nearly totally diffused within seconds. Taken together, these results suggested that the diffuse fluorescence associated with TQ treated cells is due to an activation of a cellular sialidase on the cell surface [3].

In studies where mice were pre-treated with intraperitoneal (i.p.) injections of TQ prior to being challenged with the ovalbumin (OVA) antigen, TQ was found to alter the balance of T-cell responses by decreasing the Th2 response and shifting it towards the Th1 phenotype [27, 28]. In essence, TQ treatment shifted the response from humoral to cellular immunity as evidenced by a decrease in IL-4, IL-5 and IL-13 and an increase in IFN-γ production [27]. It is noteworthy that bronchoalveolar lavage (BAL) fluid 24 h after the last OVA challenge were collected and Th2 (IL-4, IL-5, and IL-13) and Th1 (IFN-γ) cytokine levels were assessed using ELISA. OVA sensitization and challenge significantly induced the production of IL-4, IL-5, and IL-13, whereas it had a modest effect on IFN-γ production. However, when mice were treated with TQ for 5 days before airway challenge with OVA antigen, they found that not only TQ normalized the increased levels of Th2 cytokines but also induced IFN-γ production. In our studies, we collected serum before and 5 h after i.p. administration of the same dosage (3 mg/kg) of TQ as used above. We found that the TQ treatment alone during this time period produced a 1.5 to 2-fold increase in IL-4 and IL-5 in the serum and a marked increase in IL-13 (4-fold) and IFNγ (7-fold).

Studies using the mouse model of bronchial asthma also showed that TQ inhibited the generation of inflammatory indicators such as thromboxane B2 and leukotriene B4 [29]. It is believed that these properties of TQ may have resulted from TQ targeting arachidonic acid metabolism, specifically the cyclooxygenase and 5-lipoxygenase pathways through an unknown mechanism [30]. Experiments using an adjuvant-induced model of arthritis in rats showed that TQ was able to reduce inflammation in the inter-phalangeal joints of arthritic rats [31]. Treatment with TQ was also found to reduce soft tissue swelling and joint erosion as measured by arthographies. Collagen-induced production of pro-inflammatory cytokines, TNF-α and IL-1β, was reduced after TQ treatment in mice [31]. In other studies, lipopolysaccharide (LPS) stimulation of the rat basophil cell line (RBL2H3) was used as a mast cell model of inflammation since these cells resemble mucosal mast cells that mediate Th2 cell responses and contribute to chronic inflammation [28]. TNF-α pro-

duction and NFκB activation were used as indicators of inflammation caused by a Th1 cell response. When the cells were treated with TQ, there was a significant decrease in TNF-α mRNA production compared to LPS stimulated cells [28]. There was a reduction in the LPS-induced Th1 immune response with TQ treatment. In another study, it was found that LPS-treated basophil cells together with TQ had the same amount of NFκB in the cytosol and nucleus as those cells treated with LPS alone. Conversely, there was an increase in the amount of NFκB p50 homodimer binding to the promoter to repress the genes for pro-inflammatory TNF-α [28]. This decrease in TNF-α expression correlated with protection from LPS-induced colitis. The reduction of LPS-induced TNF-α with TQ treatment has also been observed *in vivo* [27, 28]. In our studies, we have observed that TQ alone can induce NFκB activation in macrophage cells similar to LPS treatment. WT and Neu1-deficient mice treated with only TQ for 5 h produced a 2-fold increase in TNF-α in the serum. It is noteworthy that TQ also induced a marked 12-fold increase in IL-1 receptor antagonist (IL-1ra), 7-fold increase in IL-1β and a 4-fold increase in IL-1α in these mice. In contrast, Neu4 knockout mice responded poorly to TQ treatment in producing any of the cytokines and chemokines measured. The IL-1 receptor antagonist (IL-1Ra) is a natural protein that competitively inhibits the binding of IL-1β and IL-1α to IL-1 receptor types I and II in humans and various animals. Unlike IL-1, binding of IL-1ra to the IL-1R1 receptor prevents the docking of the IL-1 receptor accessory proteins (IL-1R AcP) to form the heterotrimeric complex that is necessary for signalling and therefore inhibits IL-1-mediated effects [32]. Although IL-1 is a master regulator of diverse inflammatory processes in higher eukaryotes, it is the balance between interleukin-1 (IL-1) and its specific inhibitor, the IL-1 receptor antagonist (IL-1Ra), which plays a major role in the development of arthritis [33]. IL-1ra may also be the key blocker in IL-1 role in numerous autoimmune disorders including rheumatoid arthritis [32, 34, 35], diabetes [36], cardiovascular diseases [37] and cancer [38].

The above studies showing TQ acting as an anti-inflammatory agent appear to work with LPS-induced inflammation over several days of treatment. In our studies, TQ appears to have the maximum effect on macrophage cells during a 4–5 h period of stimulation. The amount of RNA encoding IL-6, TNF-α and MIP-1β was clearly elevated after 4 h of treatment with TQ in relation to the amount of mRNA for β-actin and LPS-treated positive controls. However, there was no evidence of mRNAs for these cytokines after 6 h treatment with TQ. Interestingly, we have also reported that hypomorphic cathepsin A mice with a 90% secondary Neu1 deficiency respond poorly to LPS in producing pro-inflammatory cytokines after 5 h intraperitoneal treatment compared to those elevated responses observed with the wild-type (WT), hypomorphic cathepsin A with normal Neu1 mice and Neu4-knockout (Neu4-KO) mice [1]. In contrast, the findings in this report clearly indicate that WT and the Neu1-deficient mice had a general increase in the levels of pro-inflammatory cytokines and chemokines after 5 h treatment with TQ while for the Neu4 KO mice the serum levels remained the same or decreased after treatment with TQ. Collectively, TQ induced pro-inflammatory cytokines and chemokines are partially dependent on Neu4 sialidase.

In conclusion, the data presented in this report suggest that thymoquinone (TQ), a derivative of the nutraceutical black seed (cumin) oil induces Neu4 sialidase activity in live primary macrophages and macrophage cells as well as in live HEK-TLR4/MD2 cells. This TQ-induced Neu4 sialidase activity facilitates MyD88/TLR4 complex formation and subsequent NFκB activation. Tamiflu, GPCR Gαi-sensitive pertussis toxin and broad range MMP inhibitor galardin completely block TQ-induced MyD88/TLR4 complex formation and NFκB activation. Neu4-knockout mice respond poorly to TQ-induce serum pro-inflammatory cytokines and chemokines compared to elevated responses observed with wild-type and hypomorphic cathepsin A mice with a 90% secondary Neu1 deficiency mice. Taken together, the findings establish an unprecedented activation of Neu4 sialidase on the cell surface by TQ, which circuitously targets TLR4 receptors. This report signifies for the first time an unprecedented mechanism used by TQ to target TLR4 receptors. The data supports a novel paradigm signifying that MMP-9 forms an important molecular signaling platform in complex with TLR4 receptors at the ectodomain and acts as the intermediate link for TQ-induced Neu4 activity. The data provide supporting evidence for Neu4 in complex with MMP-9 using this platform to circuitously target TLR4 receptors, enabling removal of steric hinderance for receptor association in generating a functional receptor.

Acknowledgements These studies are partially supported by grants to MRS from Natural Sciences and Engineering Research Council of Canada (NSERC). T.M.F. was a recipient of the Queen's University Research Award. A.G. and S.A. are the recipients of the Queen's Graduate Awards. P.J. is a recipient of the Queen's Graduate Award and the Robert J. Wilson Fellowship. S.R.A. was a recipient of the Queen's University Research Award, the Robert J. Wilson Fellowship and the Ontario Graduate Scholarship. Research work on the TLR transfected cell lines was supported by grants to R.B. from the 'Interuniversitaire Attractiepolen' (IAP6/18), the 'Fonds voor Wetenschappelijk Onderzoek-Vlaanderen' (FWO; grant 3G010505), and the 'Geconcerteerde Onderzoeksacties' of the Ghent University (GOA; grant 01G06B6).

We acknowledge Prof. Alexey V. Pshezhetsky and Dr. Volkan Seyrantepe from the Departments of Pediatrics and Biochemistry, Montreal University, Service de Genetique, Ste-Justine Hospital, 3175 Cote-Ste-Catherine, H3T1C5, Montreal, QC, Canada for provided us the Neu1-deficient and Neu4 knockout mice. The authors acknowledge Merry Guo in generating some of the graphic figures in this report.

Authors Contributions M.R.S. and T.M.F. wrote the paper, designed and performed experiments; P.J., A.G. and S.A. performed the TLR4 and Neu4 IP WB; K.G. assisted with the cytokine profiling; R.B. generated HEK-TLR4/MD2 cells; S.R.A. initially helped with the experiments; M.R.S. supervised the research design and the writing of the paper. All authors read and commented on the manuscript, and declare no competing financial interests.

References

1. Amith, S.R., Jayanth, P., Franchuk, S., Siddiqui, S., Seyrantepe, V., Gee, K., Basta, S., Beyaert, R., Pshezhetsky, A.V., Szewczuk, M.R.: Dependence of pathogen molecule-induced Toll-like receptor activation and cell function on Neu1 sialidase. Glycoconj. J. **26**, 1197–1212 (2009)
2. Amith, S.R., Jayanth, P., Franchuk, S., Finlay, T., Seyrantepe, V., Beyaert, R., Pshezhetsky, A.V., Szewczuk, M.R.: Neu1 desialylation of sialyl alpha-2, 3-linked beta-galactosyl residues of TOLL-like receptor 4 is essential for receptor activation and cellular signaling. Cell. Signal. **22**, 314–324 (2010)
3. Finlay, T.M., Jayanth, P., Amith, S.R., Glimour, A., Guzzo, C., Gee, K., Beyaert, R., Szewczuk, M.R.: Thymoquinone from nutraceutical black cumin oil activates Neu4 sialidase in live macrophage, dendritic, and normal and type I sialidosis human fibroblast cells via GPCR Gαi proteins and matrix metalloproteinase-9. Glycoconj. J. **27**(3), 329–348 (2010)
4. Fischer, O.M., Hart, S., Ullrich, A.: Dissecting the epidermal growth factor receptor signal transactivation pathway. Methods Mol. Biol. **327**, 85–97 (2006)
5. Lee, M.-H., Murphy, G.: Matrix metalloproteinases at a glance. J. Cell Sci. **117**, 4015–4016 (2004)
6. Le Gall, S.M., Auger, R., Dreux, C., Mauduit, P.: Regulated cell surface Pro-EGF ectodomain shedding is a zinc metalloprotease-dependent process. J. Biol. Chem. **278**, 45255–45268 (2003)
7. Murasawa, S., Mori, Y., Nozawa, Y., Gotoh, N., Shibuya, M., Masaki, H., Maruyama, K., Tsutsumi, Y., Moriguchi, Y., Shibazaki, Y., Tanaka, Y., Iwasaka, T., Inada, M., Matsubara, H.: Angiotensin II type 1 receptor-induced extracellular signal-regulated protein kinase activation is mediated by Ca2+/calmodulin-dependent transactivation of epidermal growth factor receptor. Circ. Res. **82**, 1338–1348 (1998)
8. Gooz, M., Gooz, P., Luttrell, L.M., Raymond, J.R.: 5-HT2A receptor induces ERK phosphorylation and proliferation through ADAM-17 Tumor Necrosis Factor-{alpha}-Converting Enzyme (TACE) activation and Heparin-bound Epidermal Growth Factor-like Growth Factor (HB-EGF) shedding in mesangial cells. J. Biol. Chem. **281**, 21004–21012 (2006)
9. Prenzel, N., Zwick, E., Daub, H., Leserer, M., Abraham, R., Wallasch, C., Ullrich, A.: EGF receptor transactivation by G-protein-coupled receptors requires metalloproteinase cleavage of proHB-EGF. Nature **402**, 884–888 (1999)
10. Kovacsovics-Bankowski, M., Rock, K.L.: Presentation of exogenous antigens by macrophages: analysis of major histocompatibility complex class I and II presentation and regulation by cytokines. Eur. J. Immunol. **24**, 2421–2428 (1994)
11. Ma, W., Lim, W., Gee, K., Aucoin, S., Nandan, D., Kozlowski, M., Diaz-Mitoma, F., Kumar, A.: The p38 mitogen-activated kinase pathway regulates the human interleukin-10 promoter via the activation of Sp1 transcription factor in lipopolysaccharide-stimulated human macrophages. J. Biol. Chem. **276**, 13664–13674 (2001)
12. Seyrantepe, V., Canuel, M., Carpentier, S., Landry, K., Durand, S., Liang, F., Zeng, J., Caqueret, A., Gravel, R.A., Marchesini, S., Zwingmann, C., Michaud, J., Morales, C.R., Levade, T., Pshezhetsky, A.V.: Mice deficient in Neu4 sialidase exhibit abnormal ganglioside catabolism and lysosomal storage. Hum. Mol. Genet. **17**, 1556–1568 (2008)
13. Seyrantepe, V., Hinek, A., Peng, J., Fedjaev, M., Ernest, S., Kadota, Y., Canuel, M., Itoh, K., Morales, C.R., Lavoie, J., Tremblay, J., Pshezhetsky, A.V.: Enzymatic activity of lysosomal carboxypeptidase (cathepsin) A is required for proper elastic fiber formation and inactivation of endothelin-1. Circulation **117**, 1973–1981 (2008)
14. Alatery, A., Basta, S.: An efficient culture method for generating large quantities of mature mouse splenic macrophages. J. Immunol. Methods **338**, 47–57 (2008)
15. Seyrantepe, V., Landry, K., Trudel, S., Hassan, J.A., Morales, C. R., Pshezhetsky, A.V.: Neu4, a novel human lysosomal lumen sialidase, confers normal phenotype to sialidosis and galactosialidosis cells. J. Biol. Chem. **279**, 37021–37029 (2004)
16. Ladner, K.J., Caligiuri, M.A., Guttridge, D.C.: Tumor necrosis factor-regulated biphasic activation of NF-kappa B is required for cytokine-induced loss of skeletal muscle gene products. J. Biol. Chem. **278**, 2294–2303 (2003)
17. Karin, M., Ben-Neriah, Y.: Phosphorylation meets ubiquitination: the control of NF-[kappa]B activity. Annu. Rev. Immunol. **18**, 621–663 (2000)
18. Sun, S.C., Ganchi, P.A., Ballard, D.W., Greene, W.C.: NF-kappa B controls expression of inhibitor I kappa B alpha: evidence for an inducible autoregulatory pathway. Science **259**, 1912–1915 (1993)
19. Scott, M.L., Fujita, T., Liou, H.C., Nolan, G.P., Baltimore, D.: The p65 subunit of NF-kappa B regulates I kappa B by two distinct mechanisms. Genes Dev. **7**, 1266–1276 (1993)
20. Miyamoto, S., Chiao, P.J., Verma, I.M.: Enhanced I kappa B alpha degradation is responsible for constitutive NF-kappa B activity in mature murine B-cell lines. Mol. Cell. Biol. **14**, 3276–3282 (1994)
21. Chiao, P.J., Miyamoto, S., Verma, I.M.: Autoregulation of I kappa B alpha activity. Proc. Natl. Acad. Sci. U. S. A. **91**, 28–32 (1994)
22. Arenzana-Seisdedos, F., Thompson, J., Rodriguez, M.S., Bachelerie, F., Thomas, D., Hay, R.T.: Inducible nuclear expression of newly synthesized I kappa B alpha negatively regulates DNA-binding and transcriptional activities of NF-kappa B. Mol. Cell. Biol. **15**, 2689–2696 (1995)
23. Johnson, C., Van Antwerp, D., Hope, T.J.: An N-terminal nuclear export signal is required for the nucleocytoplasmic shuttling of IkappaBalpha. EMBO J. **18**, 6682–6693 (1999)
24. Bigi, A., Morosi, L., Pozzi, C., Forcella, M., Tettamanti, G., Venerando, B., Monti, E., Fusi, P.: Human sialidase NEU4 long and short are extrinsic proteins bound to outer mitochondrial membrane and the endoplasmic reticulum, respectively. Glycobiology **20**, 148–157 (2010)
25. Hasegawa, T., Sugeno, N., Takeda, A., Matsuzaki-Kobayashi, M., Kikuchi, A., Furukawa, K., Miyagi, T., Itoyama, Y.: Role of Neu4L sialidase and its substrate ganglioside GD3 in neuronal apoptosis induced by catechol metabolites. FEBS Lett **581**, 406–412 (2007)
26. Jayanth, P., Amith, S.R., Gee, K., Szewczuk, M.R.: Neu1 sialidase and matrix metalloproteinase-9 cross-talk is essential for neurotrophin activation of Trk receptors and cellular signaling. Cell. Signal. **22**, 1193–1205 (2010)
27. El Gazzar, M., El Mezayen, R., Marecki, J.C., Nicolls, M.R., Canastar, A., Dreskin, S.C.: Anti-inflammatory effect of thymoquinone in a mouse model of allergic lung inflammation. Int. Immunopharmacol. **6**, 1135–1142 (2006)
28. El Gazzar, M.A., El Mezayen, R., Nicolls, M.R., Dreskin, S.C.: Thymoquinone attenuates proinflammatory responses in lipopolysaccharide-activated mast cells by modulating NF-kappaB nuclear transactivation. Biochim. Biophys. Acta **1770**, 556–564 (2007)

29. El Gazzar, M., El Mezayen, R., Nicolls, M.R., Marecki, J.C., Dreskin, S.C.: Downregulation of leukotriene biosynthesis by thymoquinone attenuates airway inflammation in a mouse model of allergic asthma. Biochim. Biophys. Acta **1760**, 1088–1095 (2006)
30. El Mezayen, R., El Gazzar, M., Nicolls, M.R., Marecki, J.C., Dreskin, S.C., Nomiyama, H.: Effect of thymoquinone on cyclooxygenase expression and prostaglandin production in a mouse model of allergic airway inflammation. Immunol Lett **106**, 72–81 (2006)
31. Tekeoglu, I., Dogan, A., Ediz, L., Budancamanak, M., Demirel, A.: Effects of thymoquinone (volatile oil of black cumin) on rheumatoid arthritis in rat models. Phytother. Res. **21**, 895–897 (2007)
32. Gabay, C., Lamacchia, C., Palmer, G.: IL-1 pathways in inflammation and human diseases. Nat. Rev. Rheumatol. **6**, 232–241 (2010)
33. Lamacchia, C., Palmer, G., Seemayer, C.A., Talabot-Ayer, D., Gabay, C.: Enhanced Th1 and Th17 responses and arthritis severity in mice with a deficiency of myeloid cell-specific interleukin-1 receptor antagonist. Arthritis Rheum. **62**, 452–462 (2010)
34. Molto, A., Olive, A.: Anti-IL-1 molecules: new comers and new indications. Jt. Bone Spine **77**, 102–107 (2010)
35. Fox, B.A., Stephens, M.M.: Treatment of knee osteoarthritis with Orthokine-derived autologous conditioned serum. Expert Rev. Clin. Immunol. **6**, 335–345 (2010)
36. Volarevic, V., Al-Qahtani, A., Arsenijevic, N., Pajovic, S., Lukic, M.L.: Interleukin-1 receptor antagonist (IL-1Ra) and IL-1Ra producing mesenchymal stem cells as modulators of diabetogenesis. Autoimmunity **43**, 255–263 (2010)
37. Vicenova, B., Vopalensky, V., Burysek, L., Pospisek, M.: Emerging role of interleukin-1 in cardiovascular diseases. Physiol. Res. **58**, 481–498 (2009)
38. Lavi, G., Voronov, E., Dinarello, C.A., Apte, R.N., Cohen, S.: Sustained delivery of IL-1 Ra from biodegradable microspheres reduces the number of murine B16 melanoma lung metastases. J. Control. Release **123**, 123–130 (2007)